Article

Next-Generation Drought Intensity–Duration–Frequency Curves for Early Warning Systems in Ethiopia's Pastoral Region

Getachew Tegegne [1,*], Sintayehu Alemayehu [1,2,*] , Sintayehu W. Dejene [1], Liyuneh Gebre [3], Tadesse Terefe Zeleke [1], Lidya Tesfaye [1] and Numery Abdulhamid [1]

[1] International Center for Tropical Agriculture (CIAT), Addis Ababa P.O. Box 5689, Ethiopia; s.workeneh@cgiar.org (S.W.D.); t.terefe@cgiar.org (T.T.Z.); l.tesfaye@cgiar.org (L.T.); n.abdulhamid@cgiar.org (N.A.)

[2] International Center for Tropical Agriculture (CIAT), Nairobi P.O. Box 823-00621, Kenya

[3] Ethiopian Institute of Agricultural Research, Addis Ababa P.O. Box 2003, Ethiopia; liyuneh.gebre@office.eiar.gov.et

* Correspondence: g.tegegne@cgiar.org (G.T.); S.Alemayehu@cgiar.org or sintayehu1@gmail.com (S.A.)

Abstract: The pastoral areas of Ethiopia are facing a recurrent drought crisis that significantly affects the availability of water resources for communities dependent on livestock. Despite the urgent need for effective drought early warning systems, Ethiopia's pastoral areas have limited capacities to monitor variations in the intensity–duration–frequency of droughts. This study intends to drive drought intensity–duration–frequency (IDF) curves that account for climate-model uncertainty and spatial variability, with the goal of enhancing water resources management in Borana, Ethiopia. To achieve this, the study employed quantile delta mapping to bias-correct outputs from five climate models. A novel multi-model ensemble approach, known as spatiotemporal reliability ensemble averaging, was utilized to combine climate-model outputs, exploiting the strengths of each model while discounting their weaknesses. The Standardized Precipitation Evaporation Index (SPEI) was used to quantify meteorological (3-month SPEI), agricultural (6-month SPEI), and hydrological (12-month SPEI) droughts. Overall, the analysis of historical (1990–2014) and projected (2025–2049, 2050–2074, and 2075–2099) periods revealed that climate change significantly exacerbates drought conditions across all three systems, with changes in drought being more pronounced than changes in mean precipitation. A prevailing rise in droughts' IDF features is linked to an anticipated decline in precipitation and an increase in temperature. From the derived drought IDF curves, projections for 2025–2049 and 2050–2074 indicate a significant rise in hydrological drought occurrences, while the historical and 2075–2099 periods demonstrate greater vulnerability in meteorological and agricultural systems. While the frequency of hydrological droughts is projected to decrease between 2075 and 2099 as their duration increases, the periods from 2025 to 2049 and from 2050 to 2074 are expected to experience more intense hydrological droughts. Generally, the findings underscore the critical need for timely interventions to mitigate the vulnerabilities associated with drought, particularly in areas like Borana that depend heavily on water resources availability.

Keywords: early warning system; water management; climate change; drought intensity–duration–frequency; SPEI; Borana zone; Ethiopia

1. Introduction

Ongoing greenhouse gas emissions are expected to significantly impact global climate systems, resulting in an increase in average annual global surface temperature by over 1.5 °C by the end of the 21st century in reference to the corresponding pre-industrial 1850–1900 period's average [1]. The projected intensity, duration, and frequency of droughts are expected to change significantly in the future due to climate change [2,3]. Over the past several decades, surface temperatures have risen substantially, a rising trend likely to continue unless greenhouse gas emissions are reduced [4,5]. Changes in temporal precipitation patterns are anticipated to be region-specific [1]. There will likely be a rise in the frequency and intensity of drought occurrences as temperatures rise and precipitation patterns change [6,7]. The International Disaster Database (EM-DAT) reports that, from 1998 to 2017, climate change and its related extreme events caused around 1.3 million deaths and left approximately 4.4 billion people requiring emergency assistance. Notably, 91% of these disasters stemmed from floods, heat stresses, droughts, and other extreme weather events. Global climate models (GCMs) have been employed to analyze the climate-change impact (CCI) on projected changes in drought intensity–duration–frequency (IDF).

Several studies have examined drought projections in various regions under climate change [6,8–22]. Most of these studies report a rising trend in both the severity and frequency of droughts across different regions, including tropical areas [12], the Mediterranean [19,20,22], Africa [13,15,19,20], America [19], and Asia [19]. Naumann, Alfieri [19] found that the drought frequency in the Mediterranean, Central America, south and western Asia, much of Africa, and Oceania is expected to increase by 5 to 10 times until the end of the 21st century.

The Horn of Africa, particularly Ethiopia, is currently experiencing a severe multi-year drought attributed to five consecutive failed rainy seasons, with around 23 million people facing food insecurity in Ethiopia, Kenya, and Somalia [23]. The Horn of Africa is currently grappling with a severe drought crisis, significantly affecting the availability of pasture and water for communities reliant on livestock [23,24]. In Ethiopia, the livestock sector is crucial, contributing 40% to the agricultural gross domestic product (GDP), 20% to export earnings, and 19% to the overall GDP of the country [25], yet it has been severely impacted by climate change [26]. Conflicts in pastoral areas often arise due to the scarcity of resources, particularly water and pastures. Drought has greatly impacted the availability of water and pastures in the Ethiopian pastoral region, particularly the Borana zone. The risk of droughts has escalated due to global climate change, presenting significant challenges for managing unprecedented drought conditions. These intensified droughts threaten the delicate balance of ecosystems and the livelihoods of pastoral communities that rely on consistent water sources for both domestic needs and livestock production. Rainfall in the Horn of Africa has been declining sharply since 1999, complicating agricultural decisions for crops and livestock [24]. The decline in precipitation, along with increasing temperatures and recurrent droughts, has severely impacted pastoralist communities, which represent 12–15% of Ethiopia's population and are primarily located in arid and semi-arid regions [27]. These communities contribute significantly to the national economy but are increasingly vulnerable due to climate variability. Thus, proactive climate-change impact assessments and responsive management strategies are essential for safeguarding the water resources that pastoral communities depend on.

Frequent and severe droughts have emerged as a significant climate disaster in the Borana pastoral areas, fundamentally altering the rangeland ecosystem and threatening pastoralists' and agro-pastoralists' livelihoods [26,28–30]. The key resources for livestock production, pastures and water, are intricately tied to rainfall patterns. The

ongoing drought has exacerbated the already high levels of food insecurity faced by both pastoral and agro-pastoral communities in the Borana zone. Several studies in the Borana zone have shown a consistent pattern of decreasing rainfall and increasing drought severity [31–34]. Iticha, Husen [35] emphasized that drought impacts in the Omo Ghibe River Basin and the Borana lowlands are intensified by climate change and other stressors, leading to significant livestock losses. The Borana lowlands, known for their vulnerability to climate fluctuations, have faced severe livestock losses due to increasing drought frequency and intensity [33]. Wakeyo [28] pointed out that the 2021–2022 drought led to unprecedented livestock losses in the Borena, Somali, and Afar regions. The region's population relies heavily on rainfed agriculture, which is severely impacted by below-normal rainfall, leading to crop failures and water shortages [36]. As a result, assessing the CCI on drought has emerged as a crucial research topic for enhancing our understanding of the causes and effects of global warming. Most previous studies in the Borana zone have concentrated on characterizing drought using historical data. However, understanding drought under CCI is essential for making informed decisions and preparing for future drought events. Furthermore, assessing how climate change affects drought intensity–duration–frequency (IDF) is crucial for effectively mitigating drought impacts and enhancing resilience. This study aims to fill that gap by developing drought IDF curves that account for climate-model uncertainty, spatial variability, and climate-change scenarios using bias-corrected climate-model outputs through quantile delta mapping. This approach aims to support the sustainable management of water and pasture resources and facilitate informed decision-making. Understanding the CCI on IDF and spatiotemporal dynamics of these droughts will provide critical insights that can inform timely decision-making and responses.

It is important to note that agricultural and hydrological droughts can be quantified using the Standardized Precipitation Index [37], which focuses solely on precipitation since droughts typically result from insufficient precipitation. However, rising temperatures can lead to increased evaporative losses, adversely affecting water availability. To address this, this study employs the Standardized Precipitation Evapotranspiration Index (SPEI) [22] to assess the CCI on meteorological, agricultural, and hydrological droughts in the Borana pastoral region of Ethiopia. The consequences of meteorological (3-month SPEI), agricultural (6-month SPEI), and hydrological (12-month SPEI) droughts can lead to operational drought, as noted by Pedro-Monzonís, Solera [38], as well as socio-economic drought [38,39]. In the Borana pastoral region (Figure 1), operational and socio-economic droughts are further exacerbated by population growth, unsustainable water use for livestock, and the inadequate design and management of artificial reservoirs. Hydrological droughts can significantly impact water users in the Borana zone, including the livestock sector, irrigated agriculture, ecosystems, and domestic water supplies. Conversely, meteorological droughts can negatively affect rainfed agriculture, and agricultural droughts can adversely impact both rainfed and irrigated systems. While it may be challenging to prevent the impacts of meteorological droughts due to climate change, proactive measures can be adopted to mitigate hydrological droughts [40] through investments in artificial reservoirs to store excess water during rainy seasons for use in severe dry periods [41].
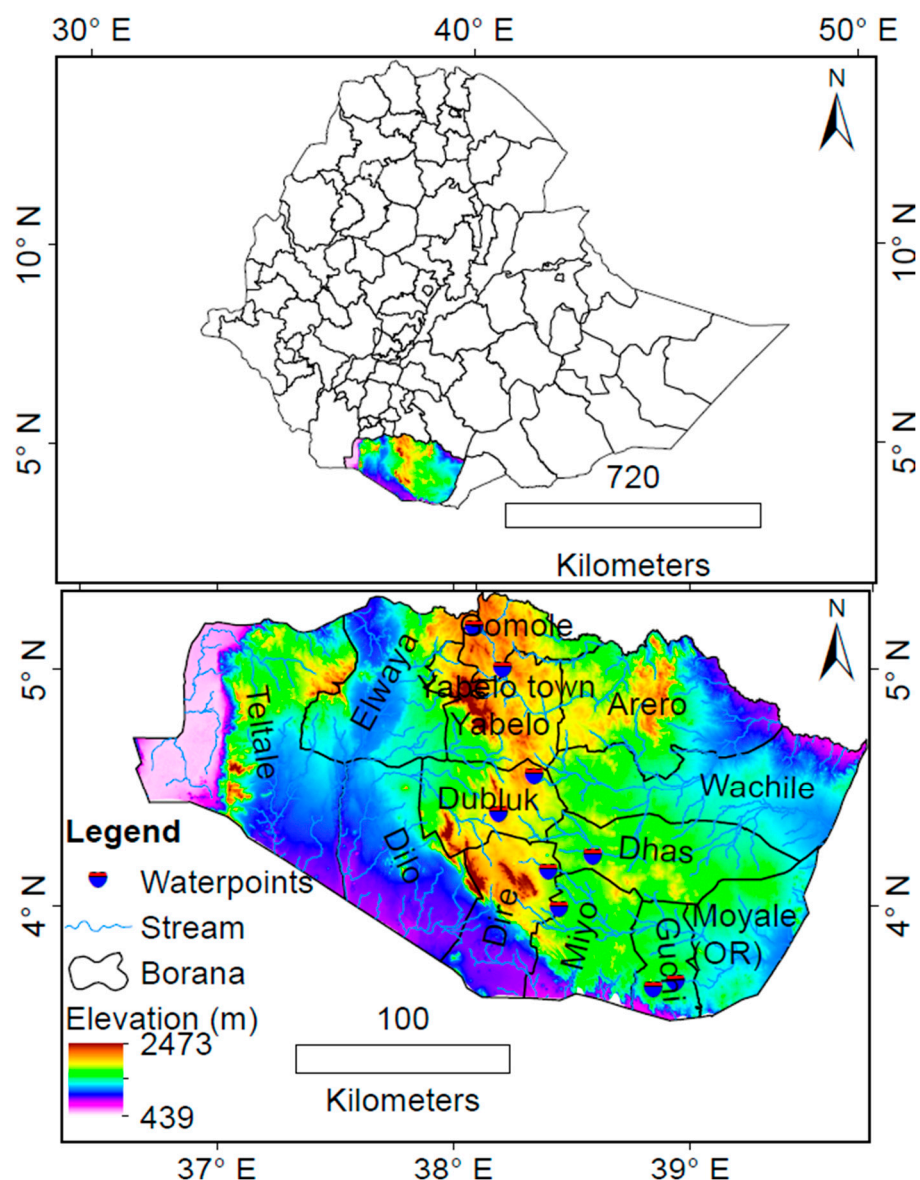
Figure 1. This map displays the location of the Borana Zone (**bottom** panel), Ethiopia (**top** panel). The water points indicate the current surface water sources available within the Borana zone. Please note that the names "Arero, Wachile, Dhas, Moyale, Guchi, Miyo, Dilo, Teltale, Elwaya, Gomole, Yabelo, Dubluk, and Dire" refer to the woredas within the study area, the Borana zone. A woreda is the third level of administrative divisions in Ethiopia, following regional states and zones.

2. Study Area and Data Description

This study was conducted in the Borana zone of the southern region of Ethiopia (Figure 1). Covering about 44,203 square kilometers, Borana is home to the largest pastoral population in the Oromia region, Southern Ethiopia. In the Borana zone, the community mainly engages in small-scale subsistence agriculture and livestock farming, both of which are highly affected by climate conditions and often struggle during droughts. Due to the area's aridity, large-scale farming is uncommon. However, the government has introduced some farming practices to help diversify income and support families. The Borana zone geographically lies between latitudes 3°30′ N and 5°25′ N and longitudes 36°40′ E and 39°45′ E. The elevation in the Borana zone ranges from 439 to 2473 m above sea level. Yabelo, the capital of Borana, is situated roughly 570 km south of Addis Ababa, and around 75% of the area is classified as lowland. The Borana zone experiences four distinct seasons: (1) Bega, which is the long dry season, lasting from December to February; (2) Belg which is the long

rainy season, from March to May; (3) Kiremt, which is a short dry spell that occurs from June to August; and (4) Meher, which is the short rainy season, from September to November. Unlike much of Ethiopia, Borana receives most of its rainfall during the Belg and Meher seasons. The climate in Borana is primarily semi-arid, with annual rainfall of 638 mm over the historical period (1986–2017) and mean annual maximum and minimum temperatures observed of 29 °C and 16 °C, respectively. Gridded data on the daily precipitation and temperature (maximum and minimum) produced through the Enhancing National Climate Services (ENACTS) initiative (4 km by 4 km) in the Borana zone for the period 1981 to 2016 were collected from the National Meteorological Agency of Ethiopia. These grided climate data were produced by ENACTS by blending the ground observations with freely available global remote satellite products.

3. Methods

3.1. Assessment of Climate-Change Impacts on Droughts

The severity and frequency of droughts can be assessed using commonly employed threshold-level methods designed to characterize drought conditions when a meteorological variable, such as rainfall or evapotranspiration, falls below a defined threshold level. This study used the SPEI [22] to analyze the frequency and intensity of meteorological (3-month SPEI), agricultural (6-month SPEI), and hydrological (12-month SPEI) droughts. The meteorological variables (precipitation and temperature) are downscaled from five GCMs, as detailed in Table 1. The quantile delta mapping (QDM) algorithm [42] is employed to adjust the GCMs daily temperature and precipitation outputs. A multi-model ensemble averaging approach was used to quantify the projected climate changes on the drought IDF. The spatiotemporal reliability ensemble averaging (ST-REA) multi-model averaging algorithm, proposed by Tegegne, Kim [43], was used to quantify the projected climate changes by combining outputs from the five GCMs through leveraging their strengths and discounting their weaknesses. The SPEI [22] is employed to quantify the droughts' frequency and intensity. The frequency and magnitude of droughts in the future periods (2025–2049, 2050–2074, and 2075–2099) are then assessed with respect to the baseline period (1990–2014). This comprehensive evaluation aims to deepen our understanding of how climate change may influence drought characteristics in the region, offering valuable insights for effective management and mitigation strategies.

Table 1. Global climate models used in this study.

No.	Model	Country	Resolution [Degree]
1	ACCESS-ESM1-5	Australia	1.875×1.25
2	BCC-CSM2-MR	China	1.1×1.1
3	CNRM-CM6-1	France	1.4×1.4
4	MIROC6	Japan	1.4×1.4
5	MRI-ESM2-0	Japan	1.125×1.125

3.2. Quantile Delta Mapping

The temperature and precipitation outputs (data) from five GCMs (Table 1) of the two commonly used Shared Socioeconomic Pathways (SSPs), 2–4.5 and 5–8.5, were downloaded from the World Climate Research program portal "https://esgf-node.ipsl.upmc.fr/search/cmip6-ipsl/ (accessed 16 January 2025)" and used in this study for drought projection. The five GCMs were selected based on their performance in previous studies on Ethiopia [44–47].

The GCMs' output is often characterized with high biases compared to the reality in the present-day scenario [42]. Johnson and Sharma [48] highlighted the importance of applying a bias correction in the GCMs' output for reliable drought projections. They found that using raw climate-model simulations led to inaccurate representations of the region. Before assessing CCI on drought, it is crucial to bias-correct precipitation and temperature outputs from GCMs based on observational datasets. Therefore, applying a bias correction to GCM outputs is a precondition for reliable climatic extreme projection estimations.

Various studies have proposed several bias correction algorithms to remove empirical cumulative distribution functions' (CDFs) biases [42,49–51]. Moreover, several studies compared the performance of different bias correction approaches in removing the CDF biases from the GCMs' output [42,52,53]. Cannon, Sobie [42] developed the quantile delta mapping (QDM) method, used in this study, to simultaneously bias-correct the CDF biases and preserve the GCM-projected variability. The GCM outputs were first spatially disaggregated to the weather station using an inverse distance interpolation technique and then bias-corrected using QDM. The QDM effectively preserves the projected changes across all quantiles of a CDF [54]. Cannon, Sobie [42] demonstrated that the QDM algorithm effectively reproduces the relative trends in climate extremes, closely aligning with the trends of raw GCMs' output. The GCMs used in this study (see Table 1) include ACCESS-ESM1-5 [55], BCC-CSM2-MR [56], CNRM-CM6-1 [57], MIROC6 [58], and MRI-ESM2-0 [59]. The QDM process involves two steps: (1) the GCM outputs are detrended by quantile and adjusted to observations through quantile mapping; and (2) the projected changes from the GCMs are superimposed on the bias-corrected climate data [42], as illustrated below.

$$\Delta_m(t) = \frac{F_{m,p}^{-1}\left[F_{m,p}^{(t)}\left(x_{m,p}(t)\right)\right]}{F_{m,h}^{-1}\left[F_{m,p}^{(t)}\left(x_{m,p}(t)\right)\right]} = \frac{x_{m,p}(t)}{F_{m,h}^{-1}\left[F_{m,p}^{(t)}\left(x_{m,p}(t)\right)\right]} \text{ for precipitation} \qquad (1)$$

$$\Delta_m(t) = x_{m,p}(t) - F_{m,h}^{-1}\left[F_{m,p}^{(t)}\left(x_{m,p}(t)\right)\right] \text{ for temperature} \qquad (2)$$

where $x_{m,p}(t)$ represents the raw GCM output at time t during the projected period, $\Delta_m(t)$ denotes the projected quantile relative changes, $F_{m,h}$ refers the CDFs of the historical simulations, and $F_{m,p}^{(t)}$ indicates the projected simulations CDFs. The bias-corrected climate simulations for the projected period are then derived by multiplying the historical corrected simulations by the relative changes, as shown below in Equations (3) (for precipitation) and (4) (for temperature):

$$\hat{x}_{m,p}(t) = F_{o,h}^{-1}\left[F_{m,h}\left(x_{m,p}(t)\right)\right]\,\Delta_m\,(t) \qquad (3)$$

$$\hat{x}_{m,p}(t) = F_{o,h}^{-1}\left[F_{m,h}\left(x_{m,p}(t)\right)\right] + \Delta_m\,(t) \qquad (4)$$

where $\hat{x}_{m,p}\,(t)$ is the projected bias-adjusted simulations at time t, and $F_{o,h}$ is the historical observed CDFs.

3.3. Spatiotemporal Reliability Ensemble Averaging

A multi-model ensemble approach enhances prediction reliability by leveraging the strengths of each climate simulator while minimizing their weaknesses [7,43,60,61]. The original Reliability Ensemble Averaging (REA) method [62] evaluates the performance of GCMs based on two key criteria: their performance to replicate observed data characteristics during the historical period and their ability to converge with other models regarding projected changes in data. This multi-model averaging assessment leads to the calculation of both performance and convergence weights. The performance weight is derived from the GCM's bias, which evaluates how accurately the GCM reproduces historical data. Con-

versely, the convergence weight reflects how closely a GCM's projected data change aligns with the ensemble mean change from multiple models. This is estimated by calculating the distance of a GCM's precipitation-change signal from the ensemble average. A key innovation of the REA approach is the incorporation of the model convergence criterion. This is particularly significant because high performance in historical simulations does not necessarily guarantee reliable future climate projections. By including convergence in the assessment, the REA method ensures that models not only perform well historically but also show consistency with the collective projections of other models. As a result, if a model's projected changes are significantly distant from the ensemble average (deemed an outlier), its performance weight is reduced accordingly.

Tegegne, Kim [43] enhanced the REA approach by introducing a spatiotemporal variability term into the weighting algorithm. This modification led to the development of the spatiotemporal reliability ensemble averaging (ST-REA) approach, which simultaneously accounts for both temporal and spatial variability in climate projections. Generally, the ST-REA weight for a specific GCM is computed as the product of two reliability terms: the performance factors—which encompass both bias (B) and variability (Var) in reproducing historical data—and the convergence factor, which is represented by the distance (D) of that model's projected changes from the ensemble mean. This comprehensive method enhances the reliability and robustness of climate-change projections, enabling more accurate assessments of future data patterns. The ST-REA considers both the spatial and temporal variability simultaneously, as shown in Equation (5).

$$w_i^{ST} = \left\{ \left[\frac{\varepsilon^{ST}}{\sqrt{\left(B_i^{ST}\right)^2 + Var_i^{ST}}} \right]^m \left[\frac{\varepsilon^{ST}}{abs\left(D_i^{ST}\right)} \right]^n \right\}^{[1/(m \times n)]} \tag{5}$$

where ε denotes the variability in the observation defined as the difference between the maximum and minimum values of the 25-year moving averages in the observations after linearly detrending the data to remove century-scale trends. The parameters m and n are used to weigh each criterion, both set to 1 in this work. w_i^{ST} indicates the ST-REA weight of *GCM i*. The letters *S* and *T* in the superscript and subscript represent the spatial and temporal variables, respectively. B_i^{ST}, Var_i^{ST}, and D_i^{ST} represent the simulation bias, variability, and distance of the target *GCM i*'s projected changes from the ensemble mean of GCMs-projected changes, respectively. B_i^{ST}, Var_i^{ST}, D_i^{ST}, and ε^{ST} can be expressed as follows:

$$B_i^{ST} = \frac{1}{J + T} \left[\Sigma_{j=1}^J \cdot \Sigma_{t=1}^T \cdot \left(X_{i,j,t} - O_{j,t} \right) \right] \tag{6}$$

$$Var_i^{ST} = \frac{1}{J + T} \left[\Sigma_{j=1}^J \cdot \Sigma_{t=1}^T \cdot \left(X_{i,j,t} - \frac{1}{J + T} \Sigma_{j=1}^J \cdot \Sigma_{t=1}^T \cdot \left(X_{i,j,t} \right) \right)^2 \right] \tag{7}$$

$$D_i^{ST} = \Delta X_i^{ST} - \frac{\sum_{i=1}^N w_i^{ST} \times \Delta X_i^{ST}}{\sum_{i=1}^N w_i^{ST}} \tag{8}$$

$$\varepsilon^{ST} = max \begin{Bmatrix} O_{1,1} & O_{1,2} & \cdots & O_{1,T} \\ O_{2,1} & O_{2,2} & \cdots & O_{2,T} \\ \vdots & \vdots & \ddots & \vdots \\ O_{J,1} & O_{J,2} & \cdots & O_{J,T} \end{Bmatrix} - min \begin{Bmatrix} O_{1,1} & O_{1,2} & \cdots & O_{1,T} \\ O_{2,1} & O_{2,2} & \cdots & O_{2,T} \\ \vdots & \vdots & \ddots & \vdots \\ O_{J,1} & O_{J,2} & \cdots & O_{J,T} \end{Bmatrix} \tag{9}$$

where *O* and *X* represent the observed and simulated data, respectively. The letters *i*, *j*, and *t* in the subscripts, respectively, represent the climate-model type, *i*, location, *j*, and time, *t*. The expressions $max\{\overline{O}_1^S, \cdots, \overline{O}_T^S\}$ and $max\{\overline{O}_1^T, \cdots, \overline{O}_J^T\}$ indicate the maximum spatial and temporal values of the average data after the data are linearly detrended, while

$min\{\overline{O}_1^S, \cdots, \overline{O}_T^S\}$ and $min\{\overline{O}_1^T, \cdots, \overline{O}_J^T\}$ represent the minimum values of the spatially and temporally averaged data, respectively, after the data are linearly detrended. Δ signifies the changes in GCM simulation, and N is the GCMs number in the analysis.

3.4. Meteorological, Agricultural, and Hydrological Droughts

CCI on droughts of different systems (i.e., meteorological, agricultural, and hydrological) were analyzed based on the ST-REA approach. The SPEI was employed to characterize the climate change risk of hydrological, meteorological, and agricultural droughts. CCI on droughts of agricultural systems often respond to meteorological anomalies over short periods, and the longer period can express the drought's impacts on the hydrological system. This is as per the United States and European drought assessment framework [63]. In this study, therefore, the CCI on meteorological, agricultural, and hydrological systems, respectively, were detected via the SPEI values at 3 months, 6 months, and 12 months. The detailed procedure for SPEI calculation can be found in the work of Vicente-Serrano, Beguería [22]. Based on the drought classification by McKee, Doesken [37], the SPEI drought intensity categories are as follows: less than -2 (extreme drought), between -1.5 and -2 (severe drought), between -1 and -1.5 (moderate drought), between -1 and 1 (normal condition), between 1 and 1.5 (moderately wet), between 1.5 and 2 (severely wet), and above 2 (extremely wet). This study used the SPEI drought intensity of less than or equal to -1 to assess the CCI on droughts. By employing this comprehensive framework, the study aimed to provide nuanced insights into how climate change is expected to affect drought characteristics across different systems, thereby guiding future research and policy decisions in resource management and climate adaptation strategies.

3.5. Drought Intensity–Duration–Frequency

This study quantified the CCI on droughts by deriving intensity–duration–frequency (IDF) curves, following the methodology by Wang, Hejazi [9]. The following steps outline the procedure used in this study to derive the IDF curves for both historical (1990–2014) and projected future periods (2025–2049, 2050–2074, and 2075–2099):

- Select drought intensity (I): Drought intensity is quantified using the SPEI. Specifically, SPEI values that are less than or equal to -1 are aggregated to compute the drought intensity.
- Determine drought duration (D): The analysis utilizes monthly data for precipitation and potential evapotranspiration to calculate drought indices. This computation is performed for durations ranging from 1 month to 24 months, allowing us to capture the variation in drought conditions over different time scales. Droughts of 1 to 3 months are short-term droughts, reflecting immediate conditions. Droughts of 3 to 6 months are useful for monitoring seasonal droughts related to agricultural impacts. Droughts of 6 to 12 months indicate moderate drought conditions that account for cumulative effects. Droughts of 12 to 24 months represent long-term drought trends, which are used for hydrological and ecological assessments. Each timescale provides insights into different aspects of droughts, helping with effective management and response strategies.
- Perform drought frequency (F): With the defined intensity and duration, the drought events frequency is assessed over a 25-year time window. This includes both baseline years (1990–2014) and future periods (2025–2049, 2050–2074, and 2075–2099). The frequency count provides insights into how often drought conditions are expected to occur under varying climate scenarios.
- Construct drought IDF curves: Finally, using both the ST-REA multi-model ensemble average and five GCMs' output, the drought IDF curves are constructed for both the

historical and projected periods. This analysis incorporates data from two emission scenarios of SSP2-4.5 and SSP5-8.5. The resulting IDF curves illustrate the relationship between drought intensity, duration, and frequency, providing a comprehensive view of how climate change may alter drought characteristics over time.

By employing this structured approach, the study aimed to derive the drought IDF curves to provide valuable insights into the anticipated changes in drought behavior due to climate change, thereby informing resource management and policy decisions in the Borana zone.

4. Results and Discussion

4.1. Projected Changes of Precipitation and Temperature

The study employed the QDM method to bias-correct precipitation and temperature data using observations from 1990 to 2005 for calibration and 2006 to 2014 for validation. The analysis confirmed that QDM effectively eliminated distributional biases in the output from GCMs. The overall projected climate-change impacts indicate a concerning trend of rising temperatures and declining precipitation in the Borana zone across all selected GCMs and future time periods (see Figure 2 for precipitation and Figure 3 for temperature). Under the SSP2-4.5 scenario, the precipitation is projected to decrease by 33.73% in 2025–2049, 32.41% in 2050–2074, and 25.52% in 2075–2099. The SSP5-8.5 scenario shows similar declines, with reductions of 33.68%, 26.67%, and 19.44% over the same periods. Detailed projections reveal variable changes in precipitation across different GCMs. For instance, the ACCESS-ESM1-5 model projects the precipitation with relative changes ranging from −64.74% to 4.64% in 2025–2049, and from −78.14% to 12.61% in 2050–2074, while showing a broader range of −64.36% to 45.61% in 2075–2099 under SSP2-4.5. Similarly, BCC-CSM2-MR indicates changes from −72.56% to 6.12% in 2025–2049 and from −75.63% to 8.69% in 2050–2074. Other models, such as CNRM-CM6-1 and MIROC6, project even steeper declines. For example, MIROC6 predicts changes from −95.83% to −1.82% in the initial period and from −89.42% to 3.55% in the next. MRI-ESM2-0 projects the precipitation with relative changes ranging from −71.78% to 17.51% in 2025–2049, with notable variability in later years. These projections highlight a consistent trend of reduced precipitation, which poses significant risks to water resources and agriculture in the Borana zone, underscoring the urgency for adaptive strategies to manage these anticipated changes.

The projected changes in average minimum and maximum temperatures indicate a significant warming trend over the coming decades, with variations depending on the scenario (Figure 3). Under SSP2-4.5, the overall average minimum temperature is modeled to increase by 0.98 °C (0.54 °C for the maximum) between 2025 and 2049. This rise reaches 1.59 °C (1.02 °C for the maximum) by 2050 to 2074 and 1.96 °C (1.24 °C for the maximum) by 2075 to 2099. For SSP5-8.5, the projections are even more pronounced (see Figure 3). The average minimum temperature is modeled to increase by 1.23 °C (0.73 °C for the maximum) from 2025 to 2049, with further increases of 2.41 °C (1.39 °C for the maximum) by 2050 to 2074, and a substantial 3.64 °C (2.23 °C for the maximum) by 2075 to 2099.

Specifically, under SSP2-4.5, minimum temperatures are projected to vary from 0.73 to 1.28 °C in 2025 to 2049, 1.27 to 2.07 °C in 2050 to 2074, and 1.59 to 2.54 °C in 2075 to 2099. Maximum temperatures will rise more modestly, ranging from 0.42 to 0.74 °C in 2025 to 2049, 0.81 to 1.28 °C in 2050 to 2074, and 0.97 to 1.57 °C in 2075 to 2099. In contrast, the SSP5-8.5 scenario shows that minimum temperatures could increase between 0.97 and 1.66 °C in 2025 to 2049, 1.94 to 3.07 °C in 2050 to 2074, and 2.94 to 4.62 °C in 2075 to 2099. Maximum temperatures under this scenario are projected to rise more significantly, from 0.62 to 0.94 °C in 2025 to 2049, 1.04 to 1.73 °C in 2050 to

2074, and 1.69 to 2.75 °C in 2075 to 2099. Generally, these projections highlight a concerning trend of increasing temperatures that could have profound implications for the pastoral and agro-pastoral sectors in the Borana zone.
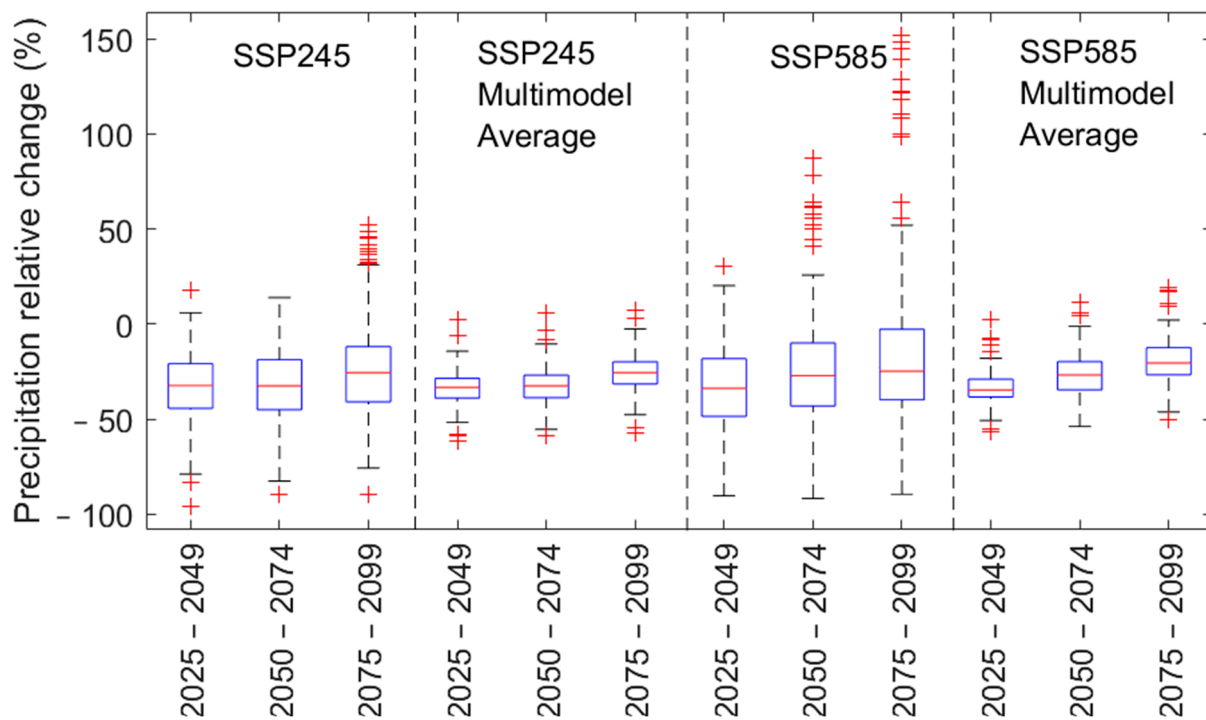

Figure 2. Projected relative changes in precipitation for the Borana zone with respect to the reference period of 1990–2014. The box represents the interquartile range, with the first quartile at the bottom and the third quartile at the top, while the red line inside the box indicates the median. The whiskers extend from the quartiles to the minimum and maximum values, with the lowest and highest data points typically outside the box representing the minimum and maximum, respectively. Red "+" symbols above and below the whiskers indicate outliers, which are unusually high or low data points.

The projected changes in average precipitation over the Borana zone indicate a significant declining trend compared to historical records, raising concerns about future drought probabilities in the region. This decline is particularly pronounced in the western parts of Borana, specifically in the Teltale and Dilo woredas, which are expected to experience the most substantial reductions in precipitation across all future time periods under both SSP2-4.5 and SSP5-8.5 (see Figure 4). In contrast, the eastern woredas, including Arero, Wachile, Dhas, Moyale, Guch, Miyo, and Dire, are projected to see relatively smaller declines in precipitation compared to the other parts of the Borana zone. However, this does not negate the overall risk; even minimal reductions can exacerbate water scarcity issues in an already vulnerable area. Please note that a woreda is the third level of administrative divisions in Ethiopia, following regional states and zones. The projected relative changes in precipitation for the Borana zone vary significantly. Under SSP2-4.5, changes are expected to range from −42.99% to −28.35% in the 2025–2049 period, −42.37% to −27.97% in 2050–2074, and −39.46% to −17.22% in 2075–2099. SSP5-8.5 shows even more drastic declines, with precipitation projected to decrease between −48.11% and −29.11% from 2025 to 2049, −36.21% to −22.73% from 2050 to 2074, and −34.91% to −13.88% from 2075 to 2099.
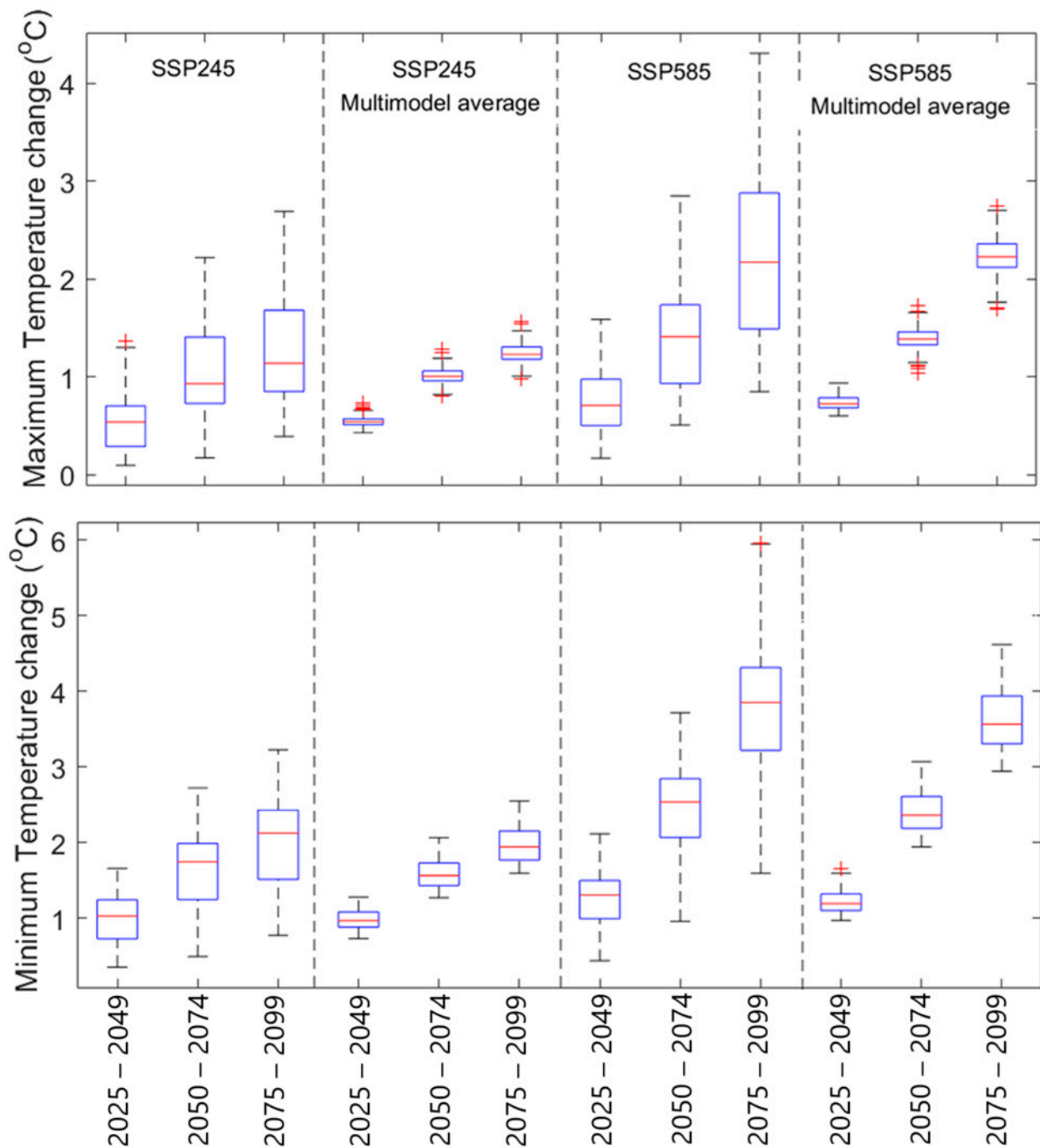
Figure 3. Maximum (**top**) and minimum (**bottom**) temperatures' projected changes relative to the baseline period (1990–2014) in the Borana zone. The box represents the interquartile range, with the first quartile at the bottom and the third quartile at the top, while the red line inside the box indicates the median. The whiskers extend from the quartiles to the minimum and maximum values, with the lowest and highest data points typically outside the box representing the minimum and maximum, respectively. The red "+" symbols above and below the whiskers indicate outliers, which are unusually high or low data points.

The substantial reductions in precipitation across different regions of Borana imply an increased likelihood of drought conditions in the future. The western woredas, facing the steepest declines, will likely experience more frequent and severe droughts, leading to significant challenges for local agriculture and livestock production, key components of the pastoralist lifestyle. As water availability diminishes, food security will be jeopardized, increasing the vulnerability of communities that rely heavily on consistent rainfall for their

livelihoods. Generally, the anticipated changes in precipitation underscore the urgent need for adaptive water management strategies and drought mitigation measures to enhance resilience in the Borana zone and support its communities in addressing the challenges posed by climate change.
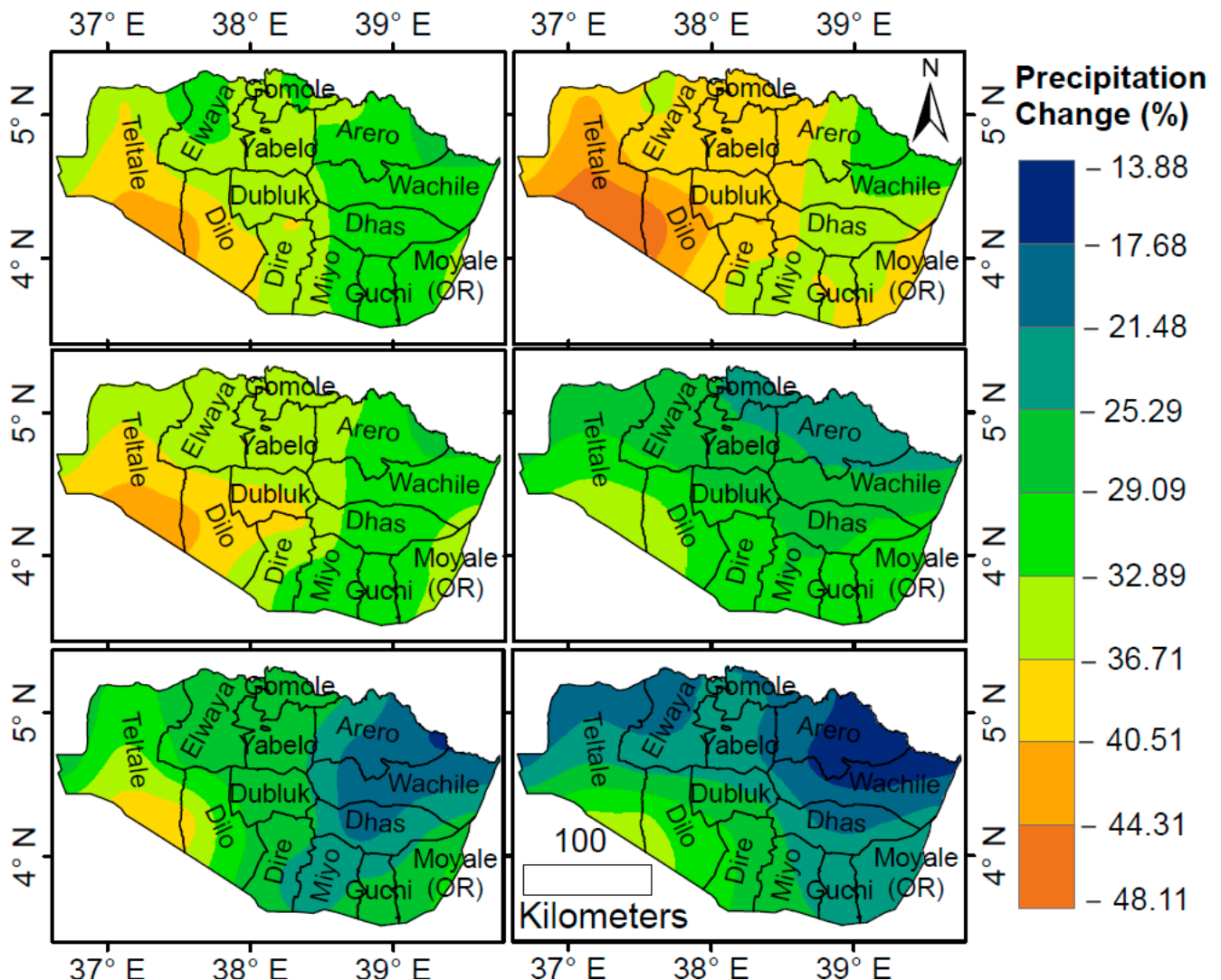

Figure 4. Projected changes in precipitation (%) over the Borana zone calculated using spatiotemporal reliability ensemble averaging (ST-REA) for the periods of 2025–2049 (**upper** row), 2050–2074 (**middle** row), and 2075–2099 (**lower** row). These changes are presented relative to the historical period of 1990–2014, under both SSP2-4.5 (**left** column) and SSP5-8.5 (**right** column). Please note that the names "Arero, Wachile, Dhas, Moyale, Guchi, Miyo, Dilo, Teltale, Elwaya, Gomole, Yabelo, Dubluk, and Dire" refer to the woredas within the study area, the Borana zone. A woreda is the third level of administrative divisions in Ethiopia, following regional states and zones.

4.2. Spatiotemporal Dynamics of Meteorological, Agricultural, and Hydrological Droughts

The intensity, frequency, severity, and spatial extent of meteorological, agricultural, and hydrological events with an SPEI value of less than or equal to −1 were used to assess the CCI on droughts in the Borana zone. Figures 5–7 show the projected variation in drought frequency for different drought durations in terms of SPEI in the Borana zone. Meteorological and agricultural droughts are influenced by precipitation anomalies over relatively short timescales, while longer SPEI periods capture the effects on hydrological droughts [63]. In the Borana zone, the range of drought frequency (estimated from five GCMs) increases as the drought duration increases from 1–3 months (toward meteorological

drought) to 3–6 months (toward agricultural drought) and 12–24 months (toward hydrological drought). The overall analysis indicates that droughts' IDF features are expected to increase in the future, primarily due to projected rises in temperature and declines in precipitation. The spatial dynamics of meteorological drought, as measured by the 3-month SPEI, indicate that the eastern regions of the Borana zone, including Yabelo, Arero, Dubluk, Dire, Miyo, Guchi, Moyale, Dhas, and Wachile, will likely experience fewer drought events compared to the western areas (see Figure 5). Specifically, the Telltale and parts of Dilo woredas are projected to face the highest drought occurrences in future periods. Overall, meteorological droughts are expected to increase across the Borana zone, with relative changes ranging from 21.81% to 391.36% in 2025–2049, 59.32% to 501.85% in 2050–2074, and 18.56% to 389.72% in 2075–2099 under SSP2-4.5. Under SSP5-8.5, these changes range from 54.36% to 454.85% in 2025–2049, −7.58% to 222.28% in 2050–2074, and −6.64% to 278.16% in 2075–2099.
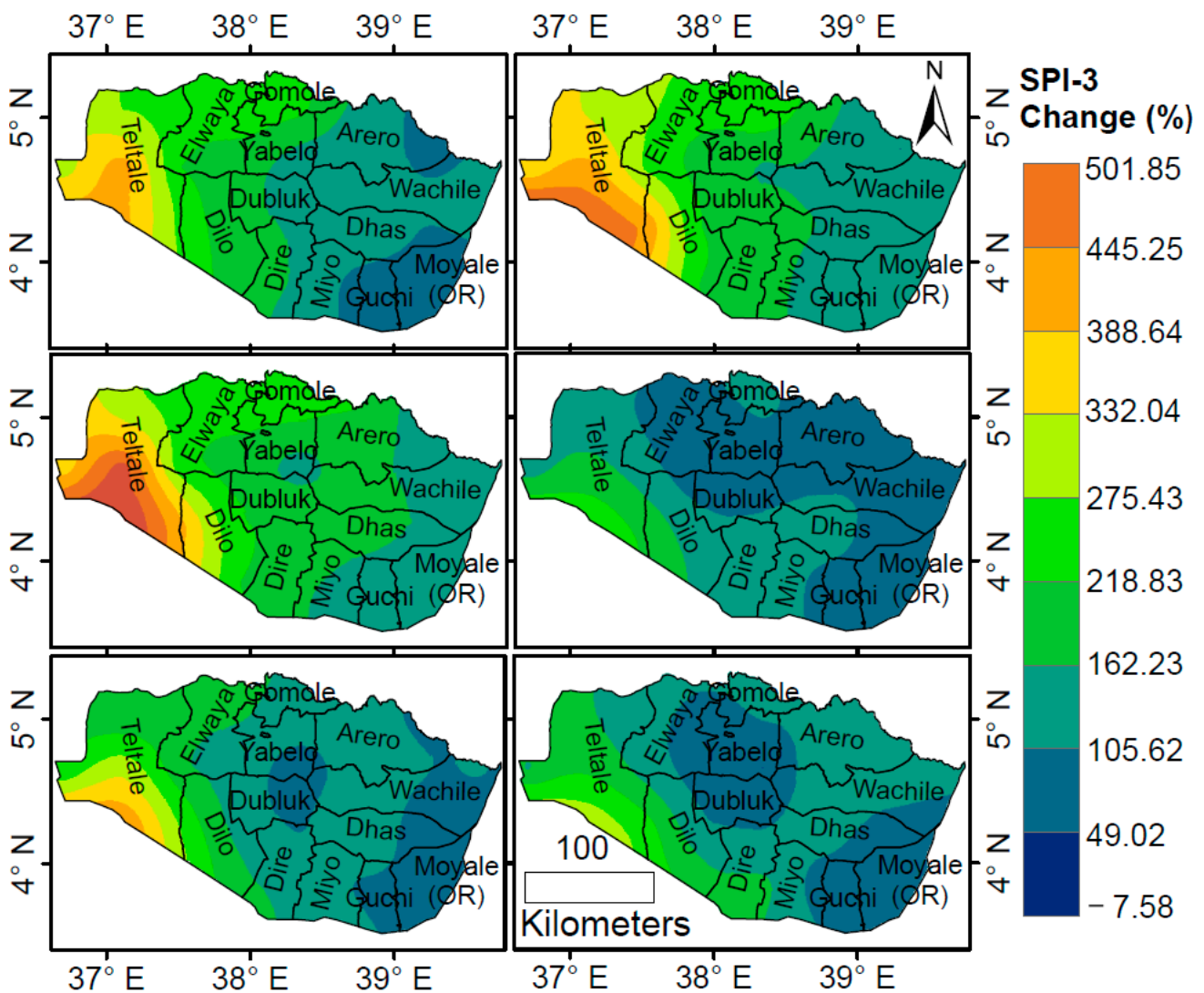

Figure 5. Meteorological droughts' (SPEI-3) projected changes calculated for the periods of 2025–2049 (first row), 2050–2074 (second row), and 2075–2099 (third row) relative to the reference period of 1990–2014. The SPEI-3 was computed and plotted for both SSP2-4.5 (**left** column) and SSP5-8.5 (**right** column). Please note that the names "Arero, Wachile, Dhas, Moyale, Guchi, Miyo, Dilo, Teltale, Elwaya, Gomole, Yabelo, Dubluk, and Dire" refer to the woredas within the study area, Borana zone. A woreda is the third level of administrative divisions in Ethiopia, following regional states and zones.
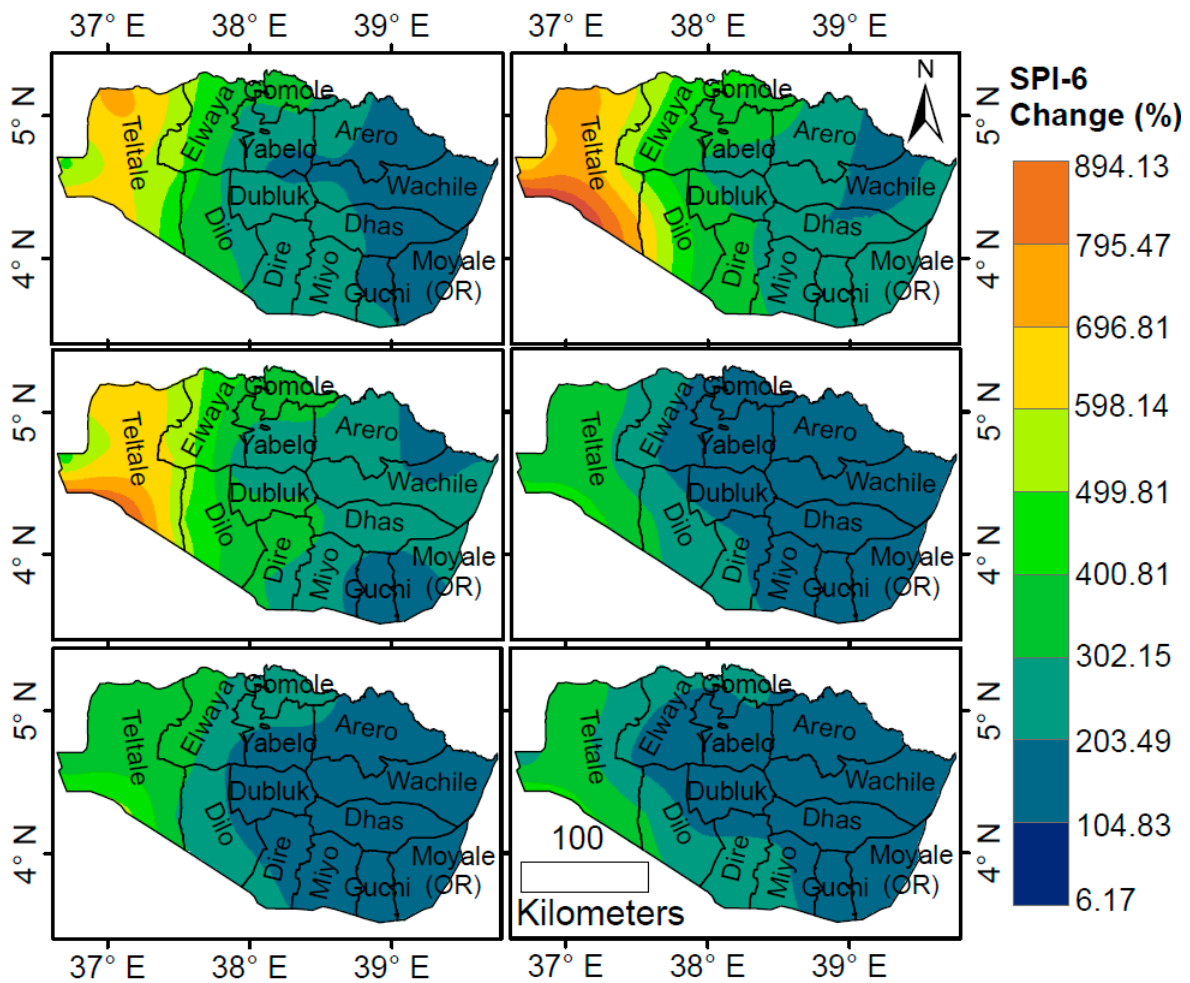
Figure 6. Agricultural droughts' (SPEI-6) projected changes calculated for the periods of 2025–2049 (first row), 2050–2074 (second row), and 2075–2099 (third row), relative to the reference period of 1990–2014. The SPEI-6 was computed and plotted for both SSP2-4.5 (**left** column) and SSP5-8.5 (**right** column). Please note that the names "Arero, Wachile, Dhas, Moyale, Guchi, Miyo, Dilo, Teltale, Elwaya, Gomole, Yabelo, Dubluk, and Dire" refer to the woredas within the study area, Borana zone. A woreda is the third level of administrative divisions in Ethiopia, following regional states and zones.

Agricultural drought, estimated by the 6-month SPEI, is projected to increase significantly throughout all regions of Borana (see Figure 6). The western areas will experience the most severe drought, with projections relative to the historical indicating changes from 49.89% to 698.62% in 2025–2049, 100.14% to 817.95% in 2050–2074, and 19.79% to 537.96% in 2075–2099 under SSP2-4.5. SSP5-8.5 presents even more alarming figures, with increases ranging from 108.06% to 894.13% in 2025–2049, 6.17% to 449.13% in 2050–2074, and 26.33% to 450.32% in 2075–2099.

Hydrological drought, assessed using the 12-month SPEI, shows that Yabelo, Arero, Miyo, Dire, and parts of Wachile will experience lower increases in drought compared to other areas (see Figure 7). In contrast, the western parts, particularly Telltale, Dilo, and Elwaya, are expected to face significant drought events. Projected relative changes in hydrological drought range from 457.61% to 1171.26% in 2025–2049, 467.24% to 1198.93% in 2050–2074, and 372.07% to 1010.95% in 2075–2099 under SSP2-4.5. Under SSP5-8.5, the increases could be even more severe, ranging from 448.23% to 1320.52% in 2025–2049, 453.19% to 1102.17% in 2050–2074, and 411.12% to 982.93% in 2075–2099. These results highlight increasing drought severity across the Borana zone. The

anticipated rise in drought events poses significant risks to agriculture, water resources, and overall food security, necessitating urgent adaptation and mitigation strategies to support the affected communities.
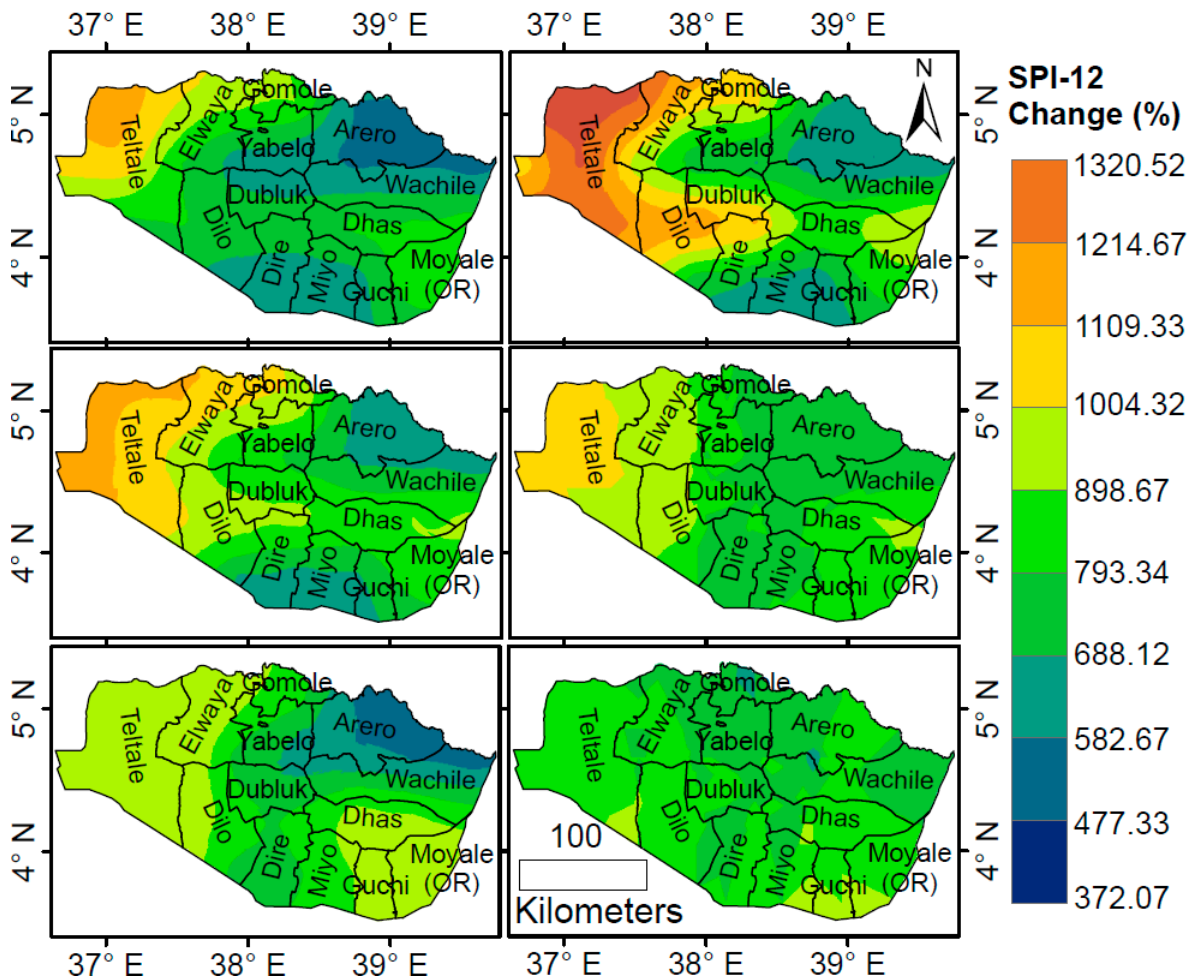

Figure 7. Hydrological droughts (SPEI-12) projected changes calculated for the periods of 2025–2049 (first row), 2050–2074 (second row), and 2075–2099 (third row), relative to the reference period of 1990–2014. The SPEI-12 was computed and plotted for both SSP2-4.5 (**left** column) and SSP5-8.5 (**right** column). Please note that the names "Arero, Wachile, Dhas, Moyale, Guchi, Miyo, Dilo, Teltale, Elwaya, Gomole, Yabelo, Dubluk, and Dire" refer to the woredas within the study area, Borana zone. A woreda is the third level of administrative divisions in Ethiopia, following regional states and zones.

Figures 8 and 9 illustrate the spatial variability of hydrological droughts at each monitoring station, assessed using the SPEI-12 for both historical and projected future periods. The sunflower plots effectively visualize the frequency of drought occurrences, with darker segments indicating a high frequency of events, while lighter segments reflect a moderate frequency. The analysis reveals a considerable projected increase in the frequency of hydrological droughts in the future compared to historical data. Notably, the majority of SPEI-12 values for the future period are expected to fall below the zero threshold, contrasting with historical values that predominantly remained above this threshold. This shift showed a heightened likelihood of frequent hydrological droughts in the Borana zone. In addition to hydrological droughts, both meteorological droughts (measured by SPEI-3) and agricultural droughts (measured by SPEI-6) are also projected to rise across all future periods relative to historical trends. This increase in drought frequency poses significant challenges for water resources, agriculture, and ecosystem health in the region.
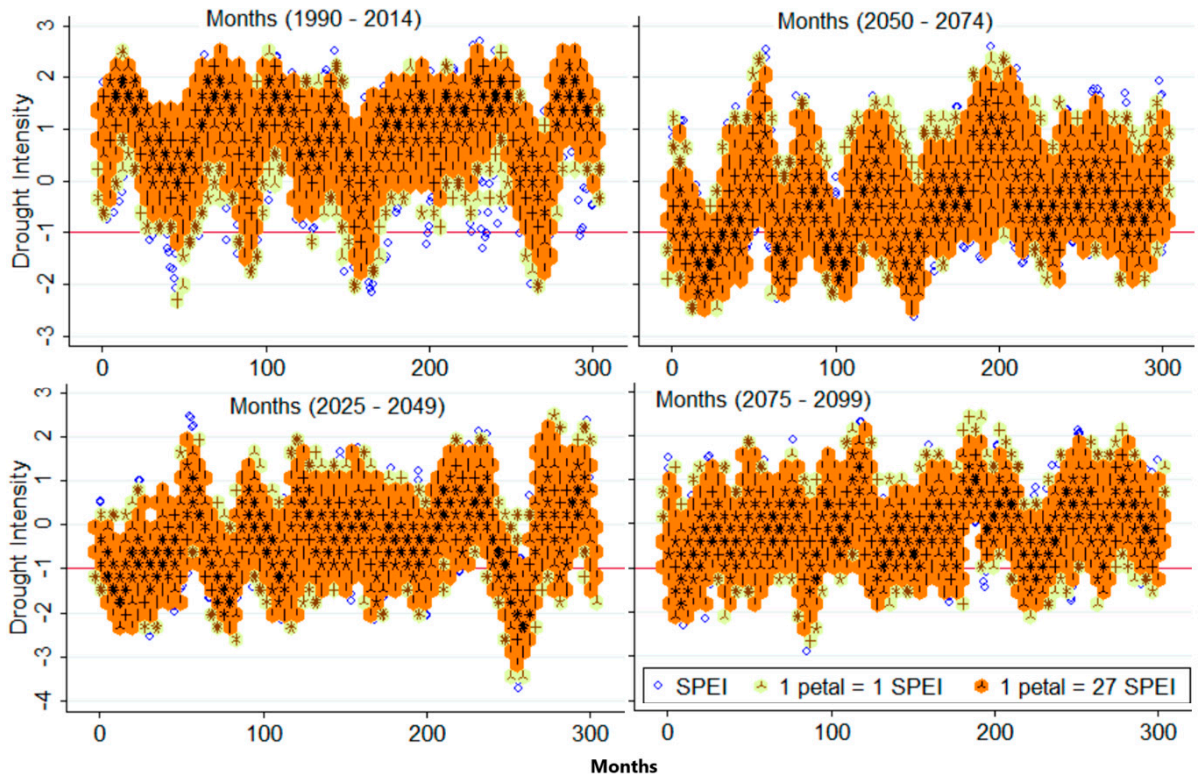
Figure 8. SPEI-12 using SSP2-4.5. Note that the range of the plot represents spatial variability based on the SPEI-12 values of all stations' data and five GCMs data. SPEI = −1 is shown in the y-axis, as it is the threshold value for the drought IDF curve development.

Figure 9. SPEI 12 using SSP5-8.5. Note that the range of the plot represents spatial variability based on the SPEI-12 values of all stations' data and five GCMs data. SPEI = −1 is shown in the y-axis, as it is the threshold value for the drought IDF curve development.
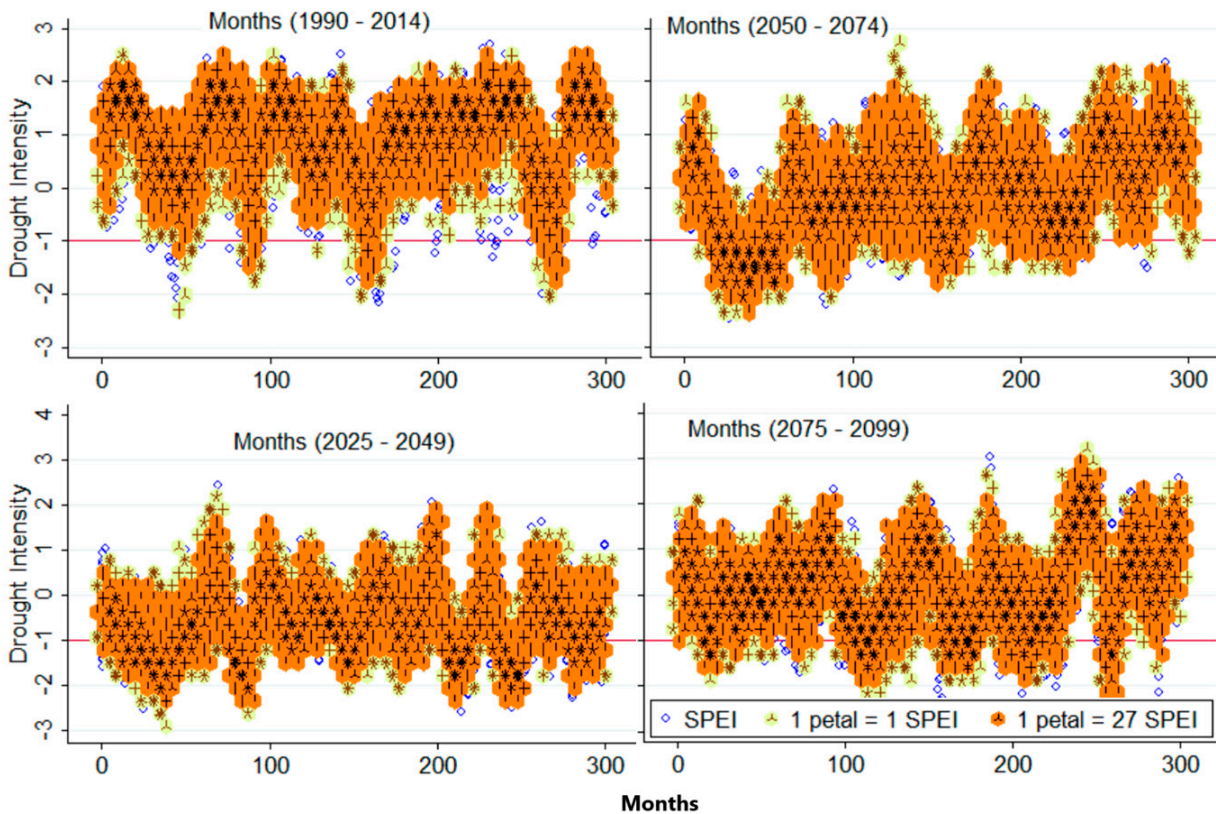
4.3. Projected Changes of Drought Intensity–Duration–Frequency (IDF) Curves

The IDF curves for meteorological (1- to 3-month SPEI), agricultural (3- to 6-month SPEI), and hydrological (12- to 24-month SPEI) droughts in the Borana zone are presented in Figures 10 and 11. These IDF curves are calculated using data from all GCMs, and they encompass values from all monitoring stations, thereby capturing both the uncertainty inherent in GCMs and the spatial variability of drought occurrences. The IDF with drought intensity of an SPEI value of less than -1 illustrates how the frequency of droughts changes over varying durations. Specifically, it depicts the relationship between the drought duration (measured in months) and drought's expected frequency. To visualize these data, density distribution sunflower plots are employed. In these plots, dark sunflowers signify high-frequency drought events, while light sunflowers represent moderate-frequency events. Each petal of a dark sunflower corresponds to 23 SPEI values, indicating a robust representation of drought events, while each petal of a light sunflower represents a single SPEI value, denoting less frequent occurrences. This visual representation aids in comprehending the frequency of droughts across different durations. The analysis reveals that the spatial variability of droughts increases as we move from meteorological (1- to 3-month SPEI) to agricultural (3- to 6-month SPEI) and finally to hydrological droughts (12- to 24-month SPEI). This progression indicates that, as drought conditions persist, their impact amplifies across different systems, affecting agricultural productivity and water resources. Projections for the periods of 2025–2049 and 2050–2074 indicate a significant rise in drought occurrences under both SSP2-4.5 and SSP5-8.5 as the drought propagates from meteorological into agricultural and hydrological systems. Interestingly, the baseline period (1990–2014) and the projected period (2075–2099) demonstrate greater vulnerability of the meteorological and agricultural systems to climate change.
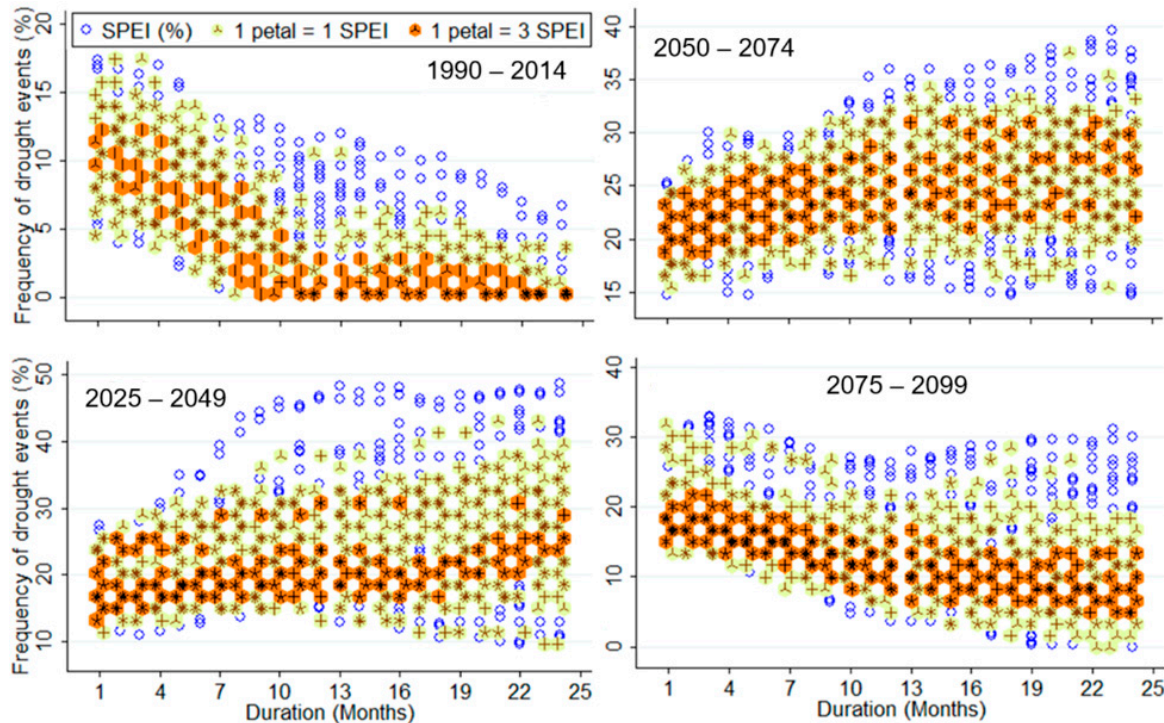

Figure 10. Drought IDF curve derived based on the data from all stations and GCMs to show the spatial variability and the uncertainty with the climate-model outputs under SSP2-4.5. Density distribution sunflower plots effectively illustrate the frequency of drought events, with dark sunflowers indicating high-frequency occurrences and light sunflowers representing moderate-density events. Each petal of a dark sunflower corresponds to 3 SPEI values, while each petal of a light sunflower reflects a single SPEI value.

Figure 11. Drought IDF curve derived based on the data from all stations and GCMs to show the spatial variability and the uncertainty with the climate-model outputs under SSP5-8.5. Density distribution sunflower plots effectively illustrate the frequency of drought events, with dark sunflowers indicating high-frequency occurrences and light sunflowers representing moderate-density events. Each petal of a dark sunflower corresponds to 3 SPEI values, while each petal of a light sunflower reflects a single SPEI value.
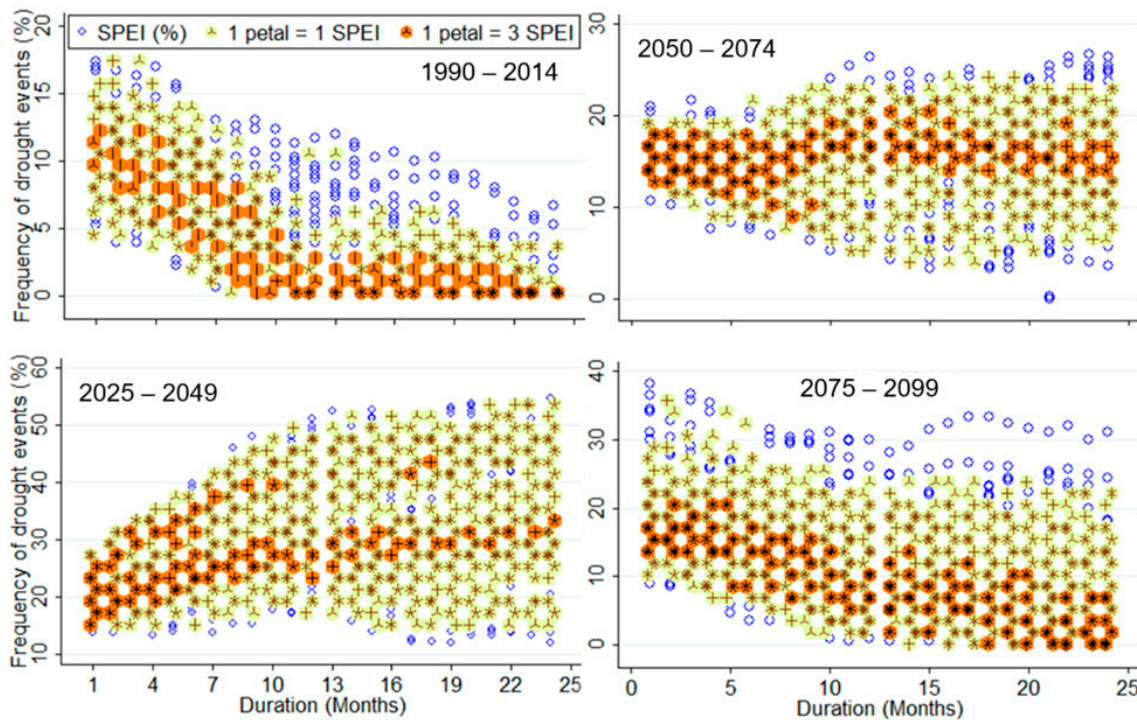
Figures 10 and 11 illustrate that the meteorological and agricultural droughts during the baseline and far-future (2075–2099) periods are more severe compared to those occurring in 2025–2049 and 2050–2074, despite the latter periods experiencing more frequent droughts. Conversely, the projected hydrological droughts are expected to be more severe during the 2025–2049 and 2050–2074 periods. The result also reveals a consistent pattern in which the frequency of agricultural and hydrological droughts decreases as the duration of the drought increases in both the historical (1990–2014) and far-future (2075–2099) periods. Furthermore, it is evident from the results that the spatial variability in drought event frequency increases with longer durations across all future periods. Generally, understanding the IDF curves and their implications for drought intensity and duration is crucial for developing effective management strategies to mitigate the CCI on water resources and agriculture in the Borana zone.

Figure 12 presents the drought IDF curves in the Borana zone, aggregated from five GCMs and all monitoring stations under SSP2-4.5 and SSP5-8.5. This analysis reveals critical insights into the future implications of drought conditions across different systems in the region. The aggregated drought indices indicate that meteorological droughts are expected to have increasingly pronounced effects on agricultural and hydrological systems during the projected periods of 2025–2049 and 2050–2074. This trend suggests a heightened probability of consecutive dry years, which poses significant risks to agricultural productivity and water availability. Specifically, as meteorological droughts persist, they are likely to exacerbate conditions in agriculture and water resources, leading to compounded impacts on food security and ecosystem health. In the historical period (1990–2014), the frequency of drought events was observed to decline as the duration of these events increased. This trend in the historical period highlights a higher frequency of meteorological and agricultural

droughts compared to hydrological droughts in the Borana zone. In the far-future periods (2075–2099), a similar frequency trend to that of the historical period is expected, suggesting that, while meteorological and agricultural droughts may frequently occur, hydrological droughts may remain less prevalent. Conversely, during the periods of 2025–2049 and 2050–2074, the frequency of droughts is projected to increase as meteorological droughts transition into agricultural and hydrological droughts. This propagation underscores a concerning trend toward consecutive dry periods, emphasizing the need for proactive management strategies.
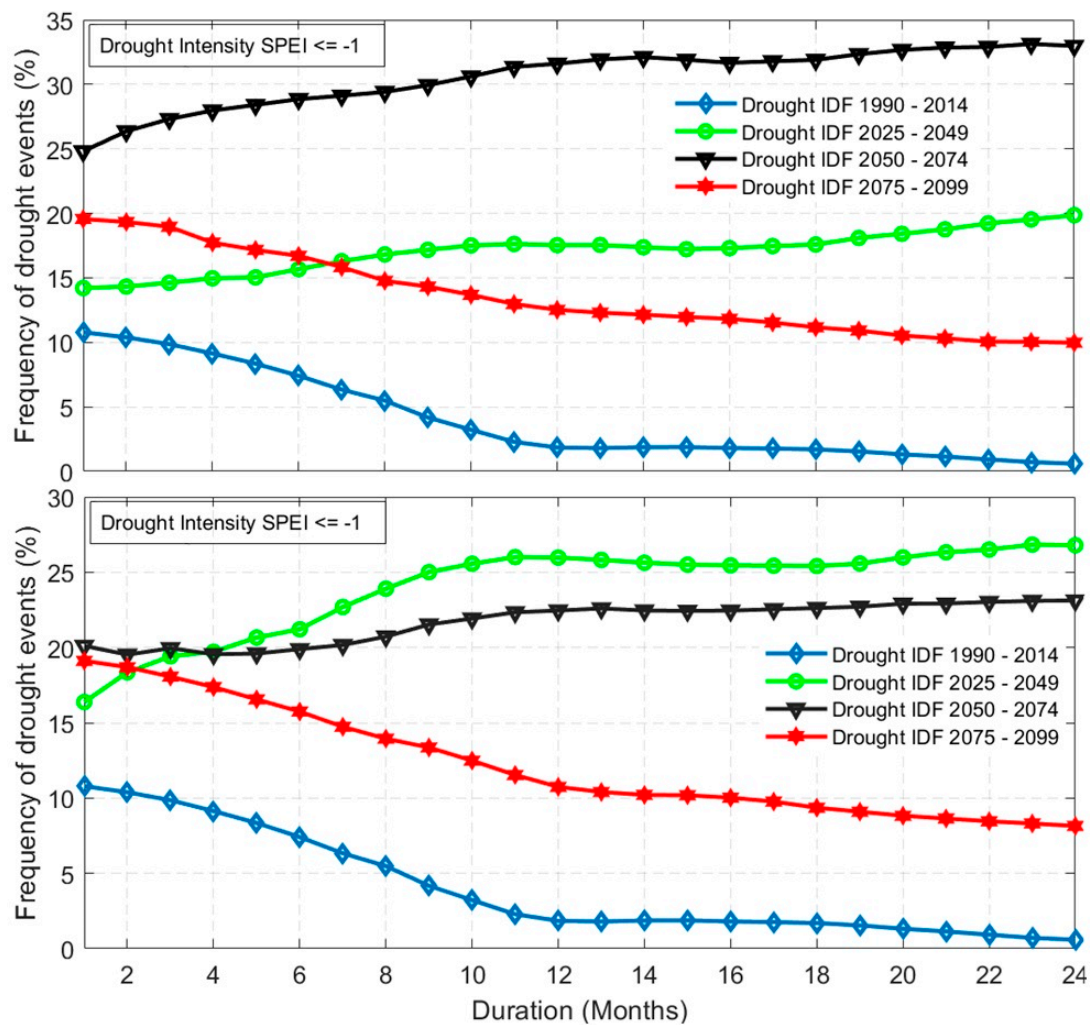

Figure 12. Drought intensity–duration–frequency (IDF) curves that are derived from the multi-model ensemble average and aggregated across all stations under SSP2-4.5 (**top**) and SSP5-8.5 (**bottom**) scenarios.

4.4. Discussion

This study analyzed the CCI on the meteorological (1- to 3-month SPEI), agricultural (3- to 6-month SPEI), and hydrological (12- to 24-month SPEI) systems by deriving drought intensity–duration–frequency (IDF) curves with an intensity of less than or equal to −1 over durations of 1 to 24 months. The results indicate a concerning increase in both the frequency and intensity of droughts across all stations, with projections suggesting that these trends will worsen in the future compared to historical data. The GCMs utilized in this study consistently predict a decline in precipitation and a rise in temperatures, contributing to an intensified drought situation in the Borana zone. The findings underscore that

climate change is significantly complicating drought management and food security in the Borana region.

Historical records show that Borana pastoralists experienced substantial livestock losses during major droughts from 1980 to 2000, with further droughts between 2005 and 2017 leading to ongoing asset depletion [64]. Rising temperatures and erratic rainfall threaten livestock by reducing the availability of pasture and water resources [65]. Previous studies revealed marked declines in mean annual rainfall during critical drought years, which adversely affected livestock populations [66]. Habte, Eshetu [67] reported an uptrend in the frequency and intensity of droughts in the Borana zone, emphasizing the need for policymakers to have access to reliable climate data to effectively address these challenges. To combat these challenges, implementing effective drought risk management strategies is crucial for alleviating poverty and improving food security [25]. A shift towards sustainable development strategies is essential for adapting to the evolving climatic conditions [68]. Adaptive strategies must be developed at household, regional, and national levels to mitigate the adverse impacts of drought.

An early warning system is vital for preparing for drought impacts, allowing for timely responses before conditions worsen [23]. To enhance Borana pastoralists' resilience through access to near-real-time water and pasture resource information, the Alliance of Bioversity International and CIAT, in collaboration with partners, developed and installed a fully working interactive and dynamic web-based digital platform (ET–Monitoring) using human-centered design (HCD). The platform provides timely and accurate information on water and forage availability to livestock producers so that they can make informed decisions. Such kinds of innovations and best experiences should be adopted and scaled up in other pastoral areas to enhance the resilience and adaptation capacity among pastoralists, as well as to support people in anticipating, responding to, and quickly recovering from crises.

Additionally, communities have developed a range of adaptations and coping strategies, including migration, livestock diversification, and emergency water and feed supplies [23]. Traditional coping mechanisms in the Borana zone include mobility, herd diversification, and forming local alliances [69,70]. Wakeyo [28] recommended promoting diversified income sources, such as agro-processing and livestock breeding technologies, as well as establishing early warning systems and small-scale water projects to bolster community resilience. Birhanu, Ambelu [26] argue that effective drought risk reduction strategies must be context-specific and incorporate local knowledge and practices. Recommendations include diversifying livestock, improving market access, and enhancing infrastructure, particularly for water resources. Timely drought warnings and meteorological information should be prioritized to strengthen the resilience of pastoral communities. While destocking is a recognized response to drought, it often serves as a last resort for herders who have strong emotional ties to their livestock [23]. Therefore, exploring alternative strategies with higher cost-benefit ratios is essential. For example, Bekele, Abera [71] demonstrated that emergency livestock feed supplementation has a higher cost–benefit ratio in Ethiopia. Mera and extremes [72] also emphasized the importance of well-planned infrastructure, adequate funding, and effective governance in addressing drought challenges. Drought responses should encompass more than just food aid; they must also include access to agricultural inputs, water sources for livestock, and the establishment of resilience programs through safety nets [25]. Such interventions can help mitigate immediate drought effects while building national capacity for climate-change adaptation.

Climate services (CSs) are increasingly employed to manage the impacts of climatic hazards [73]. Vaughan and Dessai [74] define CS as the generation and provision of climate-related information to support decision-making at all societal levels. For instance,

timely weather forecasts can enable farmers to destock and select drought-resistant crops. Tailoring CS to meet the specific needs and experiences of users can enhance decision-making quality [73]. This may require a shift from merely providing climate data to offering training on how to effectively use that data.

As droughts become more severe, the existing water infrastructure—comprising surface water points and hand-dug wells—will likely be inadequate to meet the demands for livestock and domestic use. Without the establishment of additional water sources, pastoral communities will face significant challenges in sustaining their livelihoods amid climate-induced water scarcity. Therefore, it is essential to identify and develop new water points and wells in strategic locations near communities and grazing areas. Timely planning in this regard is critical for managing the anticipated increases in drought frequency and intensity. Additionally, enhancing the storage capacity of existing water points is vital, as many are losing usability due to sediment accumulation from upstream watersheds. This gradual decline highlights the necessity for proactive measures to maintain and improve water storage facilities. Implementing integrated watershed management strategies can be pivotal in addressing sediment influx into water points. The Borana zone's grasslands are deteriorating due to multiple factors, including overgrazing and climate change [75]. By focusing on sustainable land use and soil conservation techniques in watershed areas, it is possible to reduce sediment inflow into water points and improve overall grassland health. These efforts not only enhance water quality and availability but also contribute to broader climate-change adaptation and mitigation strategies.

5. Conclusions

This study analyzed the CCI on drought conditions in the Borana zone, focusing on the intensity, frequency, severity, and spatial extent of meteorological, agricultural, and hydrological droughts. Utilizing the SPEI with a drought intensity of less than −1, the study assessed the projected variations in drought frequency across different durations. The findings reveal that drought frequency increases with duration, highlighting the sensitivity of agricultural and hydrological systems to climate change in the 2025–2049 and 2050–2074 periods. Projections indicate that, from 2025 to 2099, both temperature increases and precipitation declines will exacerbate drought conditions across the Borana zone. The spatial dynamics of drought show that eastern parts of the Borana zone, including Yabelo and Arero, are likely to experience fewer drought events compared to western areas. Notably, the Telltale and parts of Dilo woredas are projected to face the highest occurrences of drought in the future. Under SSP2-4.5 and SSP5-8.5 scenarios, the result revealed a significant increase in meteorological, agricultural, and hydrological droughts, particularly in the western regions of the Borana zone. The IDF curves generated in this study illustrate a clear progression of drought conditions, indicating that, as droughts transition from meteorological to agricultural and hydrological types, their impacts intensify. This interconnectedness underscores the need for robust adaptation strategies and community-based early warning systems to mitigate risks to agriculture, water resources, and overall food security.

As drought frequency and severity rise, livestock production and crop yields will be adversely affected, necessitating the adoption of drought-resistant crop varieties and improved water management practices. Enhanced water conservation strategies and infrastructure improvements are essential to sustaining water supplies for the pastoral community. To address these challenges, policymakers should integrate climate projections into land use and water management strategies, focusing on resilience-building measures. This includes identifying and developing new water sources, enhancing existing facilities, and implementing integrated watershed management. Implementing community-based

early warning systems and fostering collaborations between scientists and local stakeholders will further enhance drought management efforts. Without these critical interventions, the pastoral community in the Borana zone will face escalating challenges in adapting to climate change, potentially jeopardizing its livelihoods and food security. Generally, the future of water management in the Borana zone relies on a multifaceted approach that includes constructing new water sources, enhancing existing facilities, and implementing integrated watershed management.

Author Contributions: G.T. designed the methodology, analyzed the data, interpreted the results, and wrote the manuscript; S.A. supervised, reviewed, edited, and wrote the manuscript; S.W.D. reviewed, edited, and wrote the manuscript; L.G., T.T.Z., L.T. and N.A. reviewed and wrote the manuscript. All authors have read and agreed to the published version of the manuscript.

Data Availability Statement: The data used for this research are available from the first author upon request (email: g.tegegne@cgiar.org).

Conflicts of Interest: The authors declare no conflicts of interest.

References

1. IPCC. Intergovernmental Panel on Climate Change, Summary for Policymakers: Climate Change 2013. In *The Physical Science Basis, Contribution of Working Group 1 to the Fifth Assessment Report of the Intergovernmental Panel on Climate Change*; Cambridge University Press: Cambridge, UK, 2013.
2. Dai, A. Drought under global warming: A review. *WIREs Clim. Chang.* **2011**, *2*, 45–65, Corrected in *WIREs Clim. Chang.* **2012**, *3*, 617. [CrossRef]
3. Van Loon, A.F.; Stahl, K.; Di Baldassarre, G.; Clark, J.; Rangecroft, S.; Wanders, N.; Gleeson, T.; Van Dijk, A.I.; Tallaksen, L.M.; Hannaford, J.J.H.; et al. Drought in a human-modified world: Reframing drought definitions, understanding, and analysis approaches. *Hydrol. Earth Syst. Sci.* **2016**, *20*, 3631–3650. [CrossRef]
4. Mishra, A.K.; Singh, V.P. Drought modeling—A review. *J. Hydrol.* **2011**, *403*, 157–175. [CrossRef]
5. Parry, M.L. *Climate Change 2007—Impacts, Adaptation and Vulnerability: Working Group II Contribution to the Fourth Assessment Report of the IPCC*; Cambridge University Press: Cambridge, UK, 2007; Volume 4.
6. Tegegne, G.; Melesse, A.M.; Alamirew, T.J.A.R. Projected changes in extreme precipitation indices from CORDEX simulations over Ethiopia, East Africa. *Atmos. Res.* **2021**, *247*, 105156. [CrossRef]
7. Tegegne, G.; Melesse, A.M.; Worqlul, A.W. Development of multi-model ensemble approach for enhanced assessment of impacts of climate change on climate extremes. *Sci. Total. Environ.* **2020**, *704*, 135357. [CrossRef] [PubMed]
8. Raje, D.; Mujumdar, P. Hydrologic drought prediction under climate change: Uncertainty modeling with Dempster–Shafer and Bayesian approaches. *Adv. Water Resour.* **2010**, *33*, 1176–1186. [CrossRef]
9. Wang, D.; Hejazi, M.; Cai, X.; Valocchi, A.J. Climate change impact on meteorological, agricultural, and hydrological drought in central Illinois. *Water Resour. Res.* **2011**, *47*, W09527. [CrossRef]
10. Burke, E.J.; Brown, S.J. Evaluating uncertainties in the projection of future drought. *J. Hydrometeorol.* **2008**, *9*, 292–299. [CrossRef]
11. Park, C.-K.; Byun, H.-R.; Deo, R.; Lee, B.-R. Drought prediction till 2100 under RCP 8.5 climate change scenarios for Korea. *J. Hydrol.* **2015**, *526*, 221–230. [CrossRef]
12. Touma, D.; Ashfaq, M.; Nayak, M.A.; Kao, S.-C.; Diffenbaugh, N.S. A multi-model and multi-index evaluation of drought characteristics in the 21st century. *J. Hydrol.* **2015**, *526*, 196–207. [CrossRef]
13. Dai, A.J. Increasing drought under global warming in observations and models. *Nat. Clim. Change* **2013**, *3*, 52–58. [CrossRef]
14. Dai, M.; Huang, S.; Huang, Q.; Zheng, X.; Su, X.; Leng, G.; Li, Z.; Guo, Y.; Fang, W.; Liu, Y.J. Propagation characteristics and mechanism from meteorological to agricultural drought in various seasons. *J. Hydrol.* **2022**, *610*, 127897. [CrossRef]
15. Masih, I.; Maskey, S.; Mussá, F.; Trambauer, P.J.H.; sciences, e.s. A review of droughts on the African continent: A geospatial and long-term perspective. *Hydrol. Earth Syst. Sci.* **2014**, *18*, 3635–3649. [CrossRef]

16. Sheffield, J.; Wood, E.F. Characteristics of global and regional drought, 1950–2000: Analysis of soil moisture data from off-line simulation of the terrestrial hydrologic cycle. *J. Geophys. Res. Atmos.* **2007**, *112*, D1711. [CrossRef]

17. Wang, L.; Chen, W. A CMIP5 multimodel projection of future temperature, precipitation, and climatological drought in China. *Int. J. Climatol.* **2014**, *34*, 2059. [CrossRef]

18. Orlowsky, B.; Seneviratne, S.I.J.H.; Sciences, E.S. Elusive drought: Uncertainty in observed trends and short-and long-term CMIP5 projections. *Hydrol. Earth Syst. Sci.* **2013**, *17*, 1765–1781. [CrossRef]

19. Naumann, G.; Alfieri, L.; Wyser, K.; Mentaschi, L.; Betts, R.A.; Carrao, H.; Spinoni, J.; Vogt, J.; Feyen, L.J.G.R.L. Global changes in drought conditions under different levels of warming. *Geophys. Res. Lett.* **2018**, *45*, 3285–3296. [CrossRef]

20. Naumann, G.; Spinoni, J.; Vogt, J.V.; Barbosa, P.J.E.R.L. Assessment of drought damages and their uncertainties in Europe. *Environ. Res. Lett.* **2015**, *10*, 124013. [CrossRef]

21. Rhee, J.; Cho, J.J.J.o.H. Future changes in drought characteristics: Regional analysis for South Korea under CMIP5 projections. *J. Hydrometeorol.* **2016**, *17*, 437–451. [CrossRef]

22. Vicente-Serrano, S.M.; Beguería, S.; López-Moreno, J.I. A multiscalar drought index sensitive to global warming: The standardized precipitation evapotranspiration index. *J. Clim.* **2010**, *23*, 1696–1718. [CrossRef]

23. Busker, T.; de Moel, H.; van den Hurk, B.; Aerts, J.C.J. Impact-based seasonal rainfall forecasting to trigger early action for droughts. *Sci. Total Environ.* **2023**, *898*, 165506. [CrossRef] [PubMed]

24. Funk, C.; Shukla, S.; Thiaw, W.M.; Rowland, J.; Hoell, A.; McNally, A.; Husak, G.; Novella, N.; Budde, M.; Peters-Lidard, C.J.B.o.t.A.M.S. Recognizing the famine early warning systems network: Over 30 years of drought early warning science advances and partnerships promoting global food security. *Bull. Am. Meteorol. Soc.* **2019**, *100*, 1011–1027. [CrossRef]

25. World Bank. *International Development Association: Project Appraisal Document on a Proposed Credit in the Amount of SDR 121.1 Million (US$ 170 Million Equivalent) to the Federal Democratic Republic of Ethiopia for a Livestock and Fisheries Sector Development Project*; Project Appraisal Document No. PAD2396; World Bank: Washington, DC, USA, 2017.

26. Birhanu, Z.; Ambelu, A.; Berhanu, N.; Tesfaye, A.; Woldemichael, K.J. Understanding resilience dimensions and adaptive strategies to the impact of recurrent droughts in Borana Zone, Oromia Region, Ethiopia: A grounded theory approach. *Int. J. Environ. Res. Public Health* **2017**, *14*, 118. [CrossRef] [PubMed]

27. Gammino, V.M.; Diaz, M.R.; Pallas, S.W.; Greenleaf, A.R.; Kurnit, M.R. Health services uptake among nomadic pastoralist populations in Africa: A systematic review of the literature. *PLOS Neglected Trop. Dis.* **2020**, *14*, e0008474. [CrossRef] [PubMed]

28. Wakeyo, M.B. Resilience to drought and climate change disasters and its determinants in the heterogeneous pastoral Ethiopia. *Prog. Disaster Sci.* **2024**, *24*, 100366. [CrossRef]

29. Bekele, A.E.; Drabik, D.; Dries, L.; Heijman, W. Large-scale land investments, household displacement, and the effect on land degradation in semiarid agro-pastoral areas of Ethiopia. *Land Degrad. Dev.* **2021**, *32*, 777–791. [CrossRef]

30. Birhanu, Z.; Berhanu, N.; Ambelu, A. *Rapid Appraisal of Resilience to the Effects of Recurrent Droughts in Borana Zone, Southern Ethiopia*; Horn of Africa Resilience Innovation Lab (HoA RILab), Jemma University: Jimma, Ethiopia, 2015.

31. Ververs, M.-T. The East African food crisis: Did regional early warning systems function? *J. Nutr.* **2012**, *142*, 131–133. [CrossRef]

32. Kassaye, A.Y.; Shao, G.; Wang, X.; Wu, S. Quantification of drought severity change in Ethiopia during 1952–2017. *Environ. Dev. Sustain.* **2021**, *23*, 5096–5121. [CrossRef]

33. Bekele, N.; Kebede, G. Rangeland degradation and restoration in semi-arid areas of southern Ethiopia: The case of Borana rangeland. *Environ. Sci. Geogr.* **2014**, *3*, 94–103.

34. Morsy, M.; Moursy, F.I.; Sayad, T.; Shaban, S.J.P.; Geophysics, A. Climatological study of SPEI drought index using observed and CRU gridded dataset over Ethiopia. *Pure Appl. Geophys.* **2022**, *179*, 3055–3073. [CrossRef]

35. Iticha, B.; Husen, A. Adaptation to climate change using indigenous weather forecasting systems in Borana pastoralists of southern Ethiopia. *Clim. Dev.* **2019**, *11*, 564–573. [CrossRef]

36. Meza, I.; Siebert, S.; Döll, P.; Kusche, J.; Herbert, C.; Eyshi Rezaei, E.; Nouri, H.; Gerdener, H.; Popat, E.; Frischen, J.J.; et al. Global-scale drought risk assessment for agricultural systems. *Nat. Hazards Earth Syst. Sci.* **2020**, *20*, 695–712. [CrossRef]

37. McKee, T.B.; Doesken, N.J.; Kleist, J. The relationship of drought frequency and duration to time scales. In Proceedings of the 8th Conference on Applied Climatology, Anaheim, CA, USA, 17–22 January 1993; pp. 179–183.

38. Pedro-Monzonís, M.; Solera, A.; Ferrer, J.; Estrela, T.; Paredes-Arquiola, J. A review of water scarcity and drought indexes in water resources planning and management. *J. Hydrol.* **2015**, *527*, 482–493. [CrossRef]

39. Mishra, A.K.; Singh, V.P. A review of drought concepts. *J. Hydrol.* **2010**, *391*, 202–216. [CrossRef]

40. Barker, L.J.; Hannaford, J.; Chiverton, A.; Svensson, C.J. From meteorological to hydrological drought using standardised indicators. *Hydrol. Earth Syst. Sci.* **2016**, *20*, 2483–2505. [CrossRef]

41. Tegegne, G.; Kim, Y.-O. Representing inflow uncertainty for the development of monthly reservoir operations using genetic algorithms. *J. Hydrol.* **2020**, *586*, 124876. [CrossRef]

42. Cannon, A.J.; Sobie, S.R.; Murdock, T.Q. Bias correction of GCM precipitation by quantile mapping: How well do methods preserve changes in quantiles and extremes? *J. Clim.* **2015**, *28*, 6938–6959. [CrossRef]

43. Tegegne, G.; Kim, Y.O.; Lee, J. Spatiotemporal reliability ensemble averaging of multimodel simulations. *Geophys. Res. Lett.* **2019**, *46*, 12321–12330. [CrossRef]

44. Bhattacharjee, P.S.; Zaitchik, B.F. Perspectives on CMIP5 model performance in the Nile River headwaters regions. *Int. J. Climatol.* **2015**, *35*, 4262. [CrossRef]

45. Feyissa, T.A.; Demissie, T.A.; Saathoff, F.; Gebissa, A.J. Evaluation of general circulation models CMIP6 performance and future climate change over the omo river basin, Ethiopia. *Sustainability* **2023**, *15*, 6507. [CrossRef]

46. Tenfie, H.W.; Saathoff, F.; Hailu, D.; Gebissa, A.J. Selection of representative general circulation models for climate change study using advanced envelope-based and past performance approach on transboundary river basin, a case of Upper Blue Nile Basin, Ethiopia. *Sustainability* **2022**, *14*, 2140. [CrossRef]

47. Belay, H.; Melesse, A.M.; Tegegne, G. Evaluation and comparison of the performances of the CMIP5 and CMIP6 models in reproducing extreme rainfall in the Upper Blue Nile River Basin of Ethiopia. *Theor. Appl. Climatol.* **2024**, *155*, 9471–9496. [CrossRef]

48. Johnson, F.; Sharma, A. What are the impacts of bias correction on future drought projections? *J. Hydrol.* **2015**, *525*, 472–485. [CrossRef]

49. Li, H.; Sheffield, J.; Wood, E.F. Bias correction of monthly precipitation and temperature fields from Intergovernmental Panel on Climate Change AR4 models using equidistant quantile matching. *J. Geophys. Res. Atmos.* **2010**, *115*, D1010. [CrossRef]

50. Mehrotra, R.; Sharma, A. An improved standardization procedure to remove systematic low frequency variability biases in GCM simulations. *Water Resour. Res.* **2012**, *48*, W1260. [CrossRef]

51. Vrac, M. Multivariate bias adjustment of high-dimensional climate simulations: The Rank Resampling for Distributions and Dependences (R 2 D 2) bias correction. *Hydrol. Earth Syst. Sci.* **2018**, *22*, 3175. [CrossRef]

52. Teutschbein, C.; Seibert, J. Bias correction of regional climate model simulations for hydrological climate-change impact studies: Review and evaluation of different methods. *J. Hydrol.* **2012**, *456*, 12–29. [CrossRef]

53. Themeßl, M.J.; Gobiet, A.; Heinrich, G. Empirical-statistical downscaling and error correction of regional climate models and its impact on the climate change signal. *Clim. Change* **2012**, *112*, 449–468. [CrossRef]

54. Tegegne, G.; Melesse, A.M. Comparison of trend preserving statistical downscaling algorithms toward an improved precipitation extremes projection in the headwaters of blue nile river in Ethiopia. *Environ. Process.* **2021**, *8*, 59–75. [CrossRef]

55. Ziehn, T.; Chamberlain, M.A.; Law, R.M.; Lenton, A.; Bodman, R.W.; Dix, M.; Stevens, L.; Wang, Y.-P.; Srbinovsky, J. The Australian Earth System Model: ACCESS-ESM1.5. *J. South. Hemisph. Earth Syst. Sci.* **2020**, *70*, 193–214. [CrossRef]

56. Wu, T.; Lu, Y.; Fang, Y.; Xin, X.; Li, L.; Li, W.; Jie, W.; Zhang, J.; Liu, Y.; Zhang, L.; et al. The Beijing Climate Center Climate System Model (BCC-CSM): The main progress from CMIP5 to CMIP6. *Geosci. Model Dev.* **2019**, *12*, 1573–1600. [CrossRef]

57. Voldoire, A.; Saint-Martin, D.; Sénési, S.; Decharme, B.; Alias, A.; Chevallier, M.; Colin, J.; Guérémy, J.F.; Michou, M.; Moine, M.P.; et al. Evaluation of CMIP6 deck experiments with CNRM-CM6-1. *J. Adv. Model. Earth Syst.* **2019**, *11*, 2177–2213. [CrossRef]

58. Tatebe, H.; Ogura, T.; Nitta, T.; Komuro, Y.; Ogochi, K.; Takemura, T.; Sudo, K.; Sekiguchi, M.; Abe, M.; Saito, F.; et al. Description and basic evaluation of simulated mean state, internal variability, and climate sensitivity in MIROC6. *Geosci. Model Dev.* **2019**, *12*, 2727–2765. [CrossRef]

59. Kawai, H.; Yukimoto, S.; Koshiro, T.; Oshima, N.; Tanaka, T.; Yoshimura, H.; Nagasawa, R. Significant improvement of cloud representation in the global climate model MRI-ESM2. *Geosci. Model Dev.* **2019**, *12*, 2875–2897. [CrossRef]

60. Tegegne, G.; Melesse, A.M. Multimodel ensemble projection of hydro-climatic extremes for climate change impact assessment on water resources. *Water Resour. Manag.* **2020**, *34*, 3019–3035. [CrossRef]

61. Tegegne, G.; Mellesse, A.M. Multimodel ensemble projection of precipitation over South Korea using the reliability ensemble averaging. *Theor. Appl. Clim.* **2023**, *151*, 1205–1214. [CrossRef]

62. Giorgi, F.; Mearns, L.O. Calculation of average, uncertainty range, and reliability of regional climate changes from AOGCM simulations via the "reliability ensemble averaging"(REA) method. *J. Clim.* **2002**, *15*, 1141–1158. [CrossRef]

63. Stagge, J.H.; Kohn, I.; Tallaksen, L.M.; Stahl, K. Modeling drought impact occurrence based on meteorological drought indices in Europe. *J. Hydrol.* **2015**, *530*, 37–50. [CrossRef]

64. Shibru, M.; Opere, A.; Omondi, P.; Gichaba, M. Understanding physical climate risks and their implication for community adaptation in the borana zone of southern Ethiopia using mixed-methods research. *Sci. Rep.* **2023**, *13*, 6916. [CrossRef] [PubMed]

65. Coppock, D.L.; Gebru, G.; Desta, S.; Mesele, S.; Tezerra, S. Are cattle die-offs predictable on the Borana plateau. In *Global Livestock Collaborative Research Support Program*; University of California at Davis: Davis, CA, USA, 2008.

66. Ayal, D.Y.; Radeny, M.; Desta, S.; Gebru, G. Climate variability, perceptions of pastoralists and their adaptation strategies: Implications for livestock system and diseases in Borana zone. *Int. J. Clim. Change Strateg. Manag.* **2018**, *10*, 596–615. [CrossRef]

67. Habte, M.; Eshetu, M.; Maryo, M.; Andualem, D.; Legesse, A. Effects of climate variability on livestock productivity and pastoralists perception: The case of drought resilience in Southeastern Ethiopia. *Veter-Anim. Sci.* **2022**, *16*, 100240. [CrossRef] [PubMed]

68. Anita, W.; Dominic, M.; Neil, A. *Climate Change and Agriculture Impacts, Adaptation and Mitigation: Impacts, Adaptation and Mitigation*; OECD Publishing: Paris, France, 2010.

69. Deresse, T.; Daba, B. Assessing the Influence of Drought and Coping Strategy Focus Pastoralist: The Case of Melka Sodda Woreda, West Guji Zone, Southern Ethiopia. *J. Environ. Hazards* **2021**, *5*, 4.
70. Wario, H.T.; Roba, H.G.; Kaufmann, B. Responding to mobility constraints: Recent shifts in resource use practices and herding strategies in the Borana pastoral system, southern Ethiopia. *J. Arid. Environ.* **2016**, *127*, 222–234. [CrossRef]
71. Bekele, G.; Abera, T. *Livelihoods-based Drought Response in Ethiopia: Impact Assessment of Livestock Feed Supplementation*; Feinstein International Center, Tufts University and Save the Children US, Addis Ababa: Washington, DC, USA, 2008.
72. Mera, G.A. Drought and its impacts in Ethiopia. *Weather. Clim. Extrem.* **2018**, *22*, 24–35. [CrossRef]
73. Muller, L.C.; Schaafsma, M.; Mazzoleni, M.; Van Loon, A.F. Responding to climate services in the context of drought: A systematic review. *Clim. Serv.* **2024**, *35*, 100493. [CrossRef]
74. Vaughan, C.; Dessai, S. Climate services for society: Origins, institutional arrangements, and design elements for an evaluation framework. *WIREs Clim. Chang.* **2014**, *5*, 587–603. [CrossRef] [PubMed]
75. Daba, B.; Mammo, S. Rangeland degradation and management practice in Ethiopia: A systematic review paper. *Environ. Sustain. Indic.* **2024**, *23*, 100413. [CrossRef]